Responsive and reconfigurable endoskeletal emulsions

Eric M. Furst & Tamás Prileszky
Department of Chemical and Biomolecular Engineering &
Center for Molecular and Engineering Thermodynamics
University of Delaware

Alexandra V. Bayles*
*current address: UCSB Chemical Engineering

Patrick T. Spicer
Department of Chemical Engineering
University of New South Wales

Workshop on Complex Fluids in Biological Systems
Banff, July 23–27, 2018

Funding acknowledgments
Procter & Gamble
NSF CBET–1336132

Responsive and reconfigurable endoskeletal emulsions

Eric M. Furst & Tamás Prileszky
Department of Chemical and Biomolecular Engineering &
Center for Molecular and Engineering Thermodynamics
University of Delaware

Alexandra V. Bayles*
*current address: UCSB Chemical Engineering

Patrick T. Spicer
Department of Chemical Engineering
University of New South Wales

75 µm

Workshop on Complex Fluids in Biological Systems
Banff, July 23–27, 2018

Funding acknowledgments

Procter & Gamble
NSF CBET–1336132

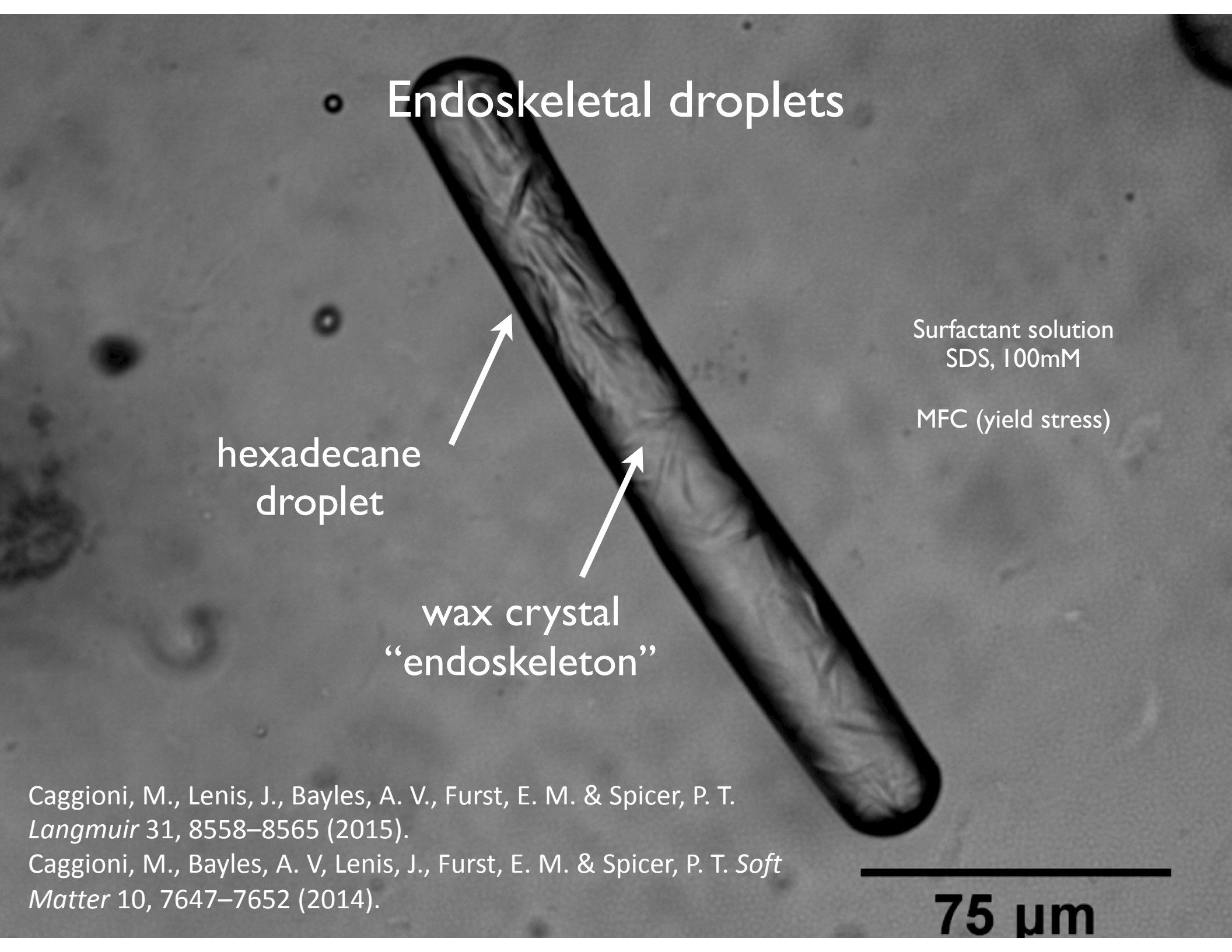

Caggioni, M., Lenis, J., Bayles, A. V., Furst, E. M. & Spicer, P. T. *Langmuir* 31, 8558–8565 (2015).
Caggioni, M., Bayles, A. V, Lenis, J., Furst, E. M. & Spicer, P. T. *Soft Matter* 10, 7647–7652 (2014).

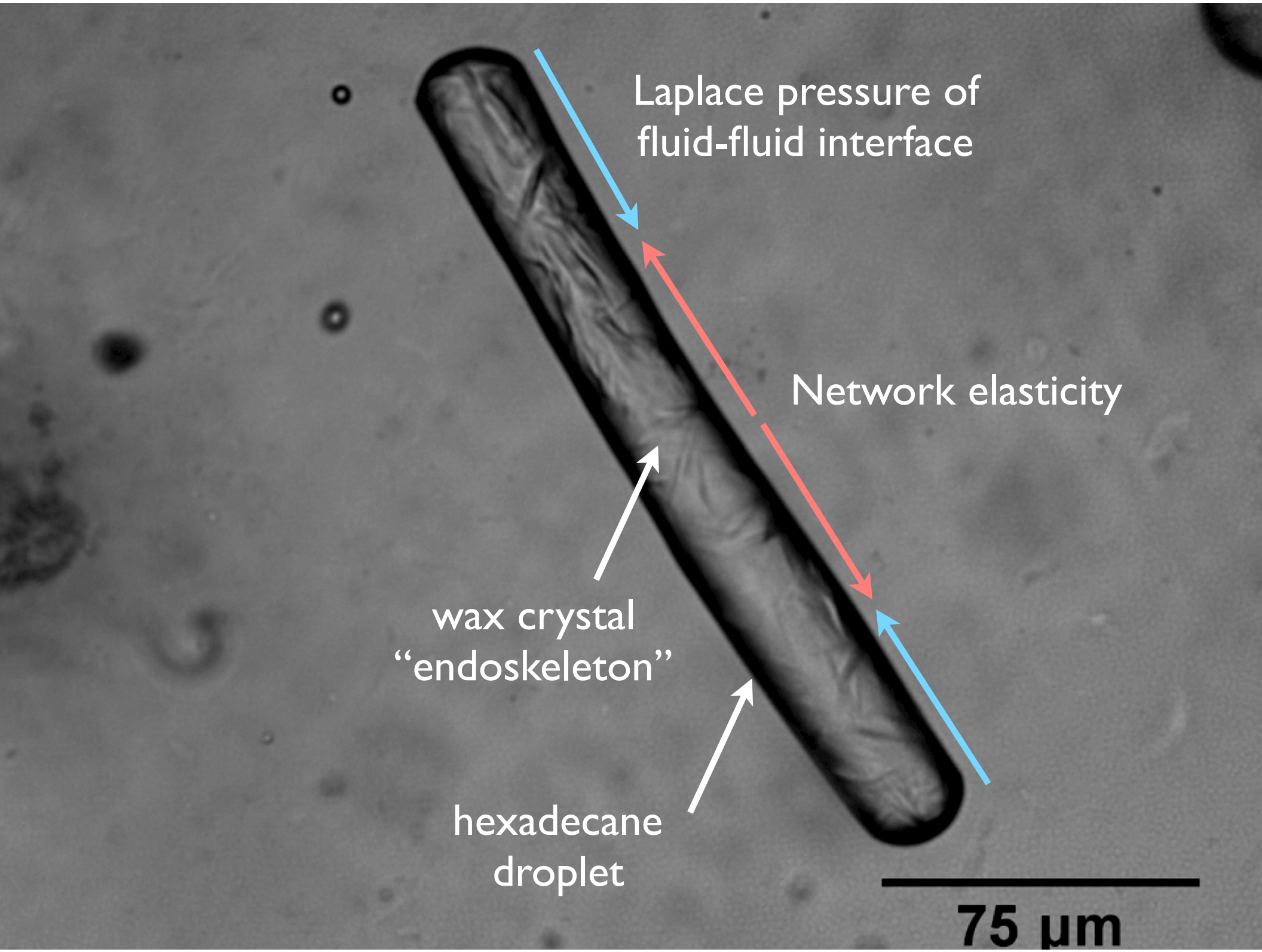
Laplace pressure of
fluid-fluid interface
Network elasticity
wax crystal
"endoskeleton"
hexadecane
droplet
75 µm

Cell shape and motility

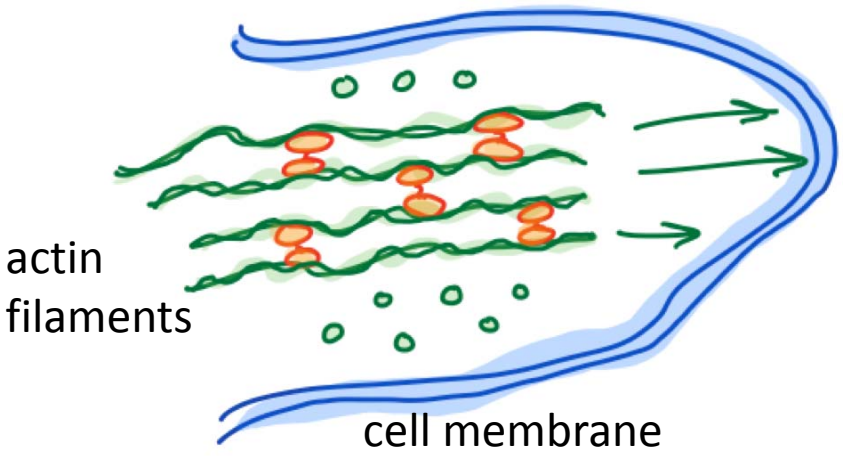

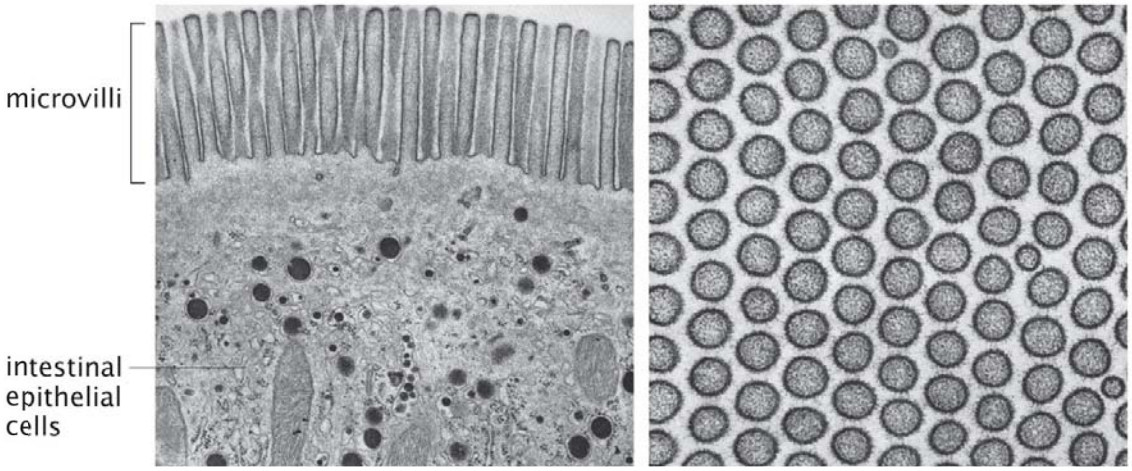

Theriot Lab, Stanford

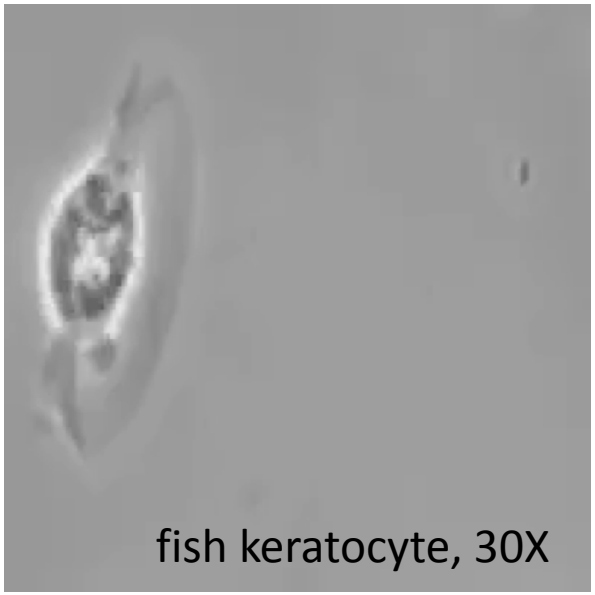

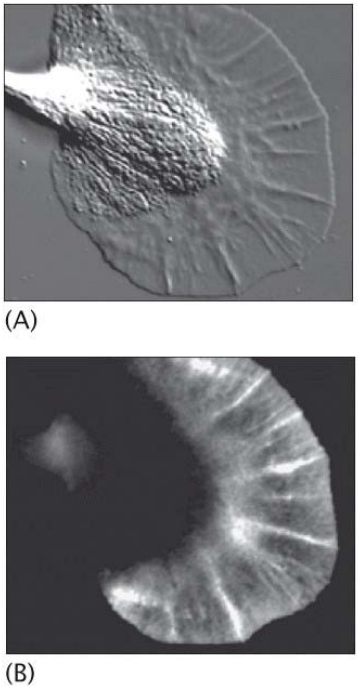

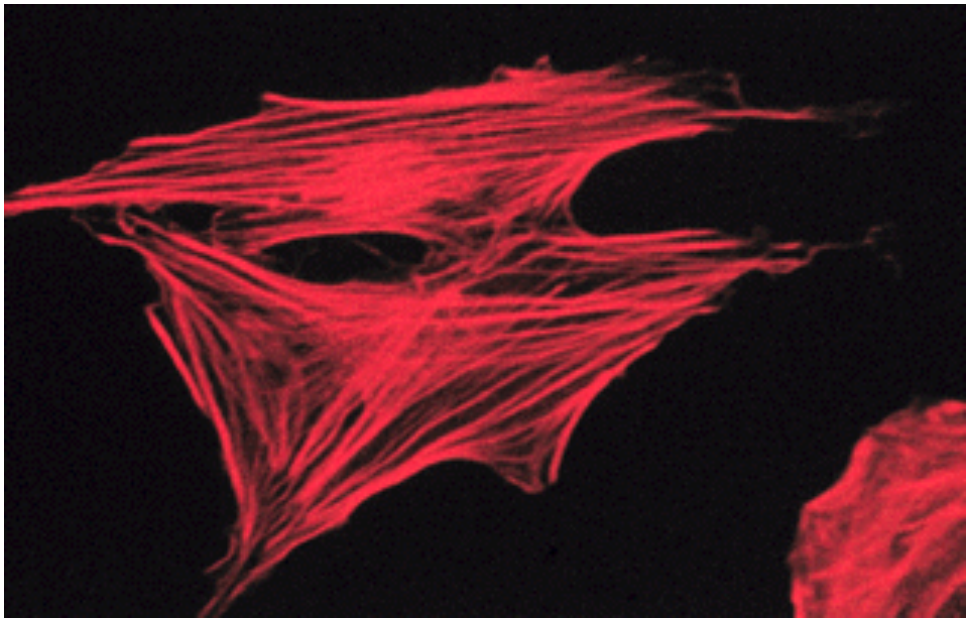

D. Bray. *Cell Movements*. Garland Science, New York, 2001.
Rob Phillips, Jane Kondev, Julie Theriot, Hernan Garcia, *Physical Biology of the Cell*, Garland Science, New York, 2013

Fluid emulsions are common delivery vehicles for active ingredients

agriculture / crop protection

consumer products

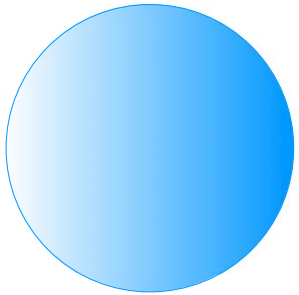

Emulsion or droplet
– surface tension, minimum area

Advantages of shape anisotropy for deposition

Delivery / transport

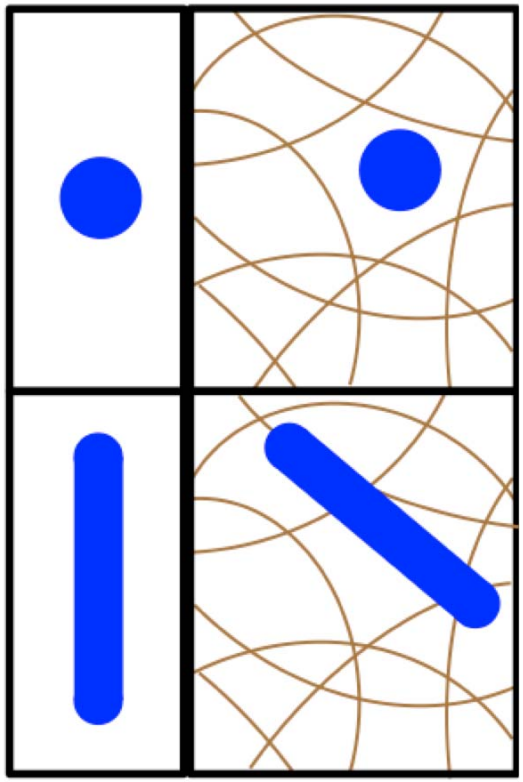

better filtration, higher collision cross-section

Retention

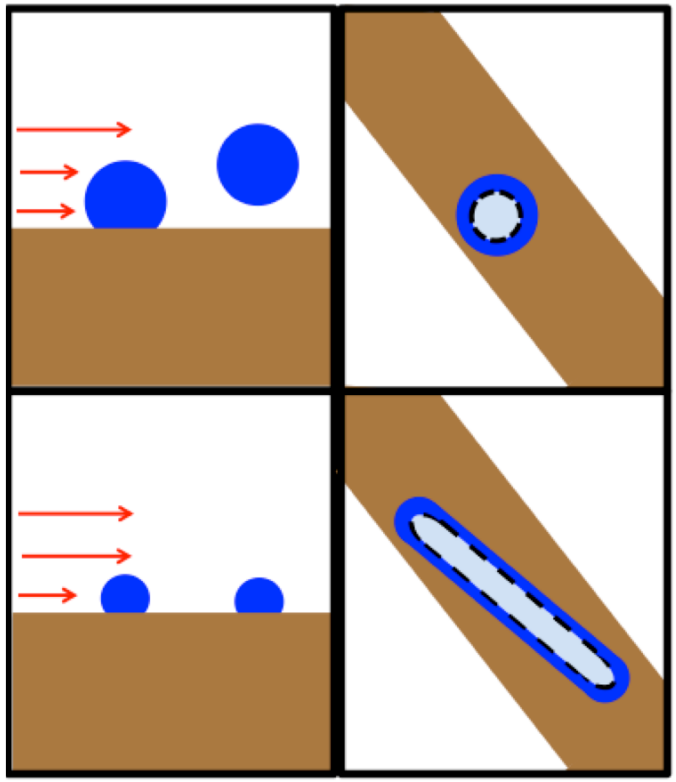

greater contact, adhesion, shape reconfiguration

Spicer et al. U.S. Patent No. 9,597,648 B2

Capillary molding

Endoskeletal droplets
60–80 wt% petrolatum: branched alkanes (n > 25)
20–40 wt% hexadecane: linear alkane (n = 16)

Aqueous phase
10 mM sodium dodecyl sulfate (SDS)

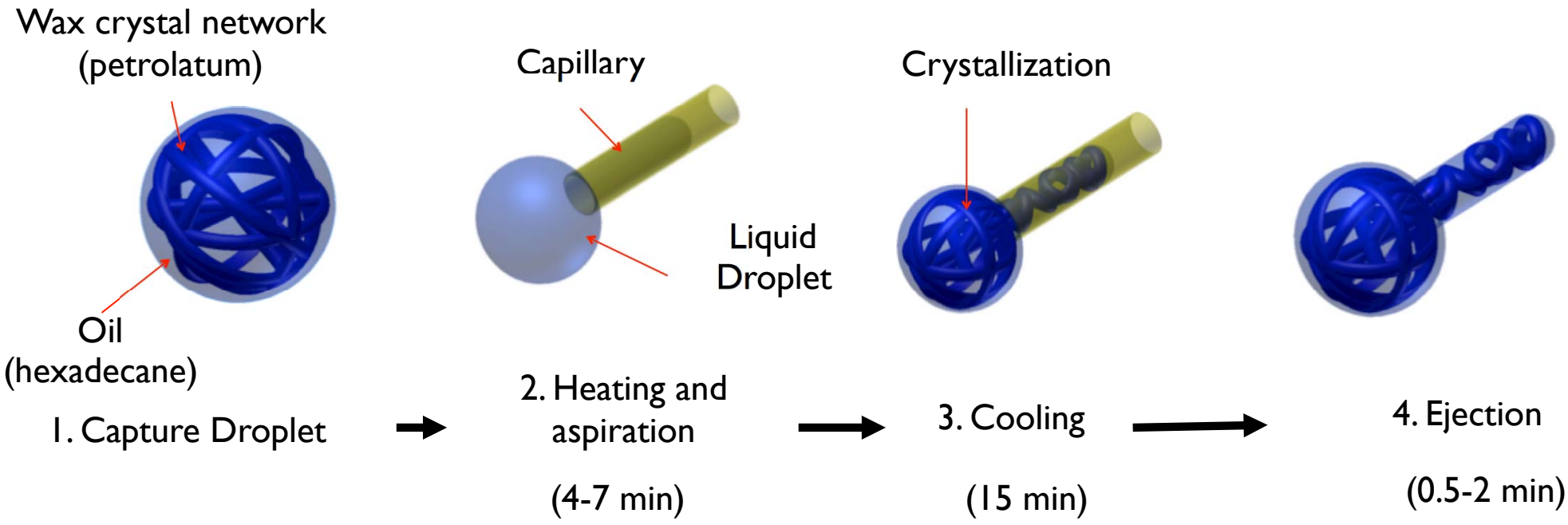

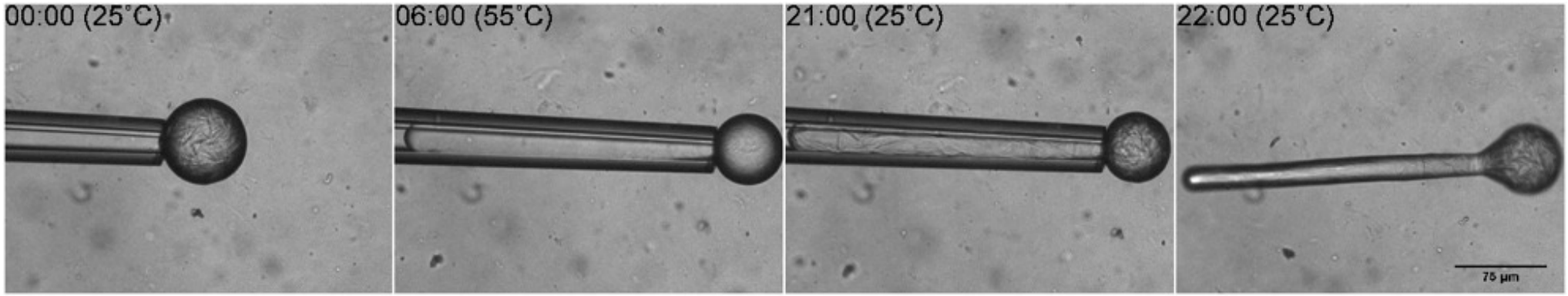

Structured droplet geometries

produced by capillary molding

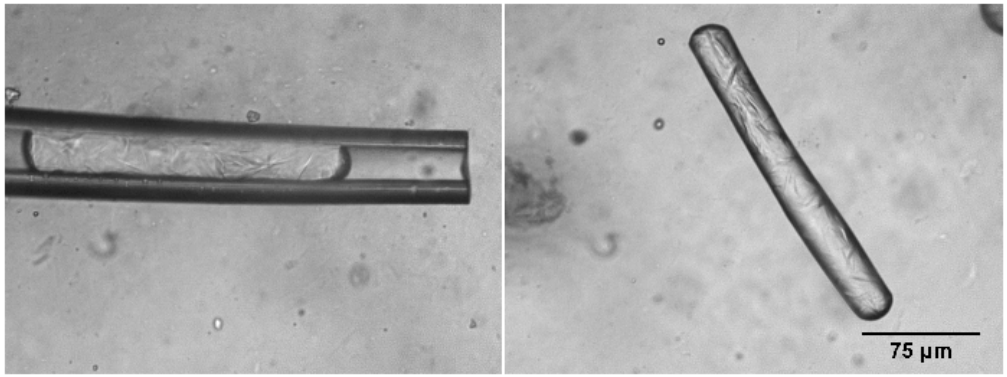

"Spherocylinder"

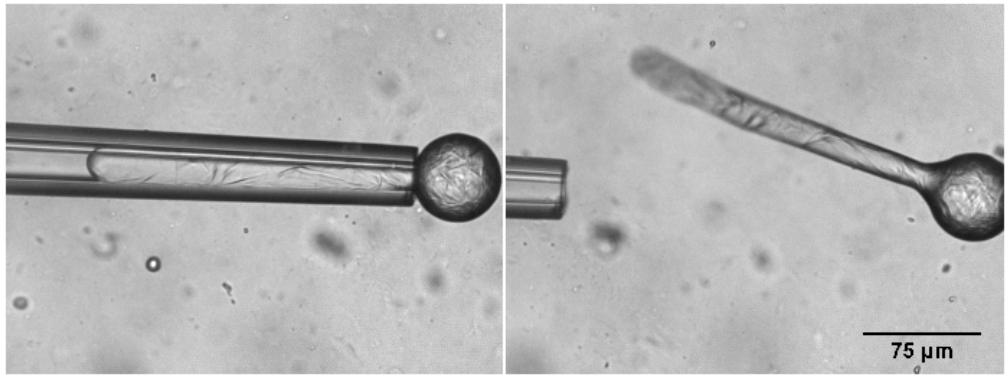

"Ball and stick"

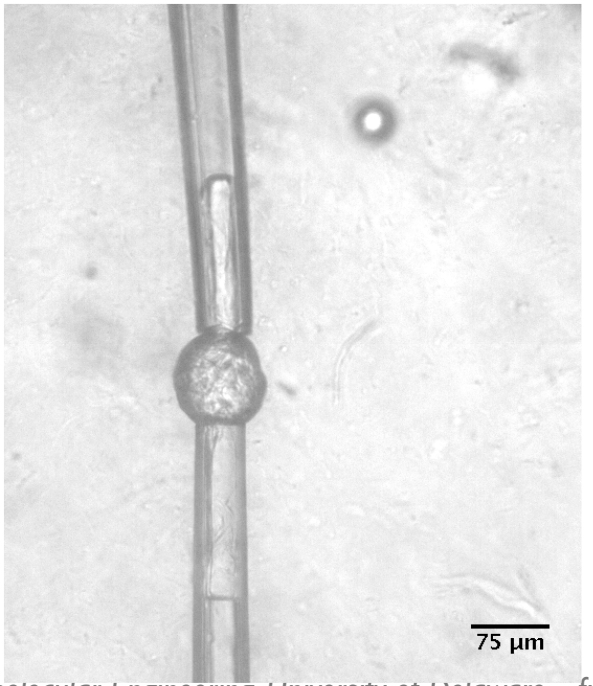

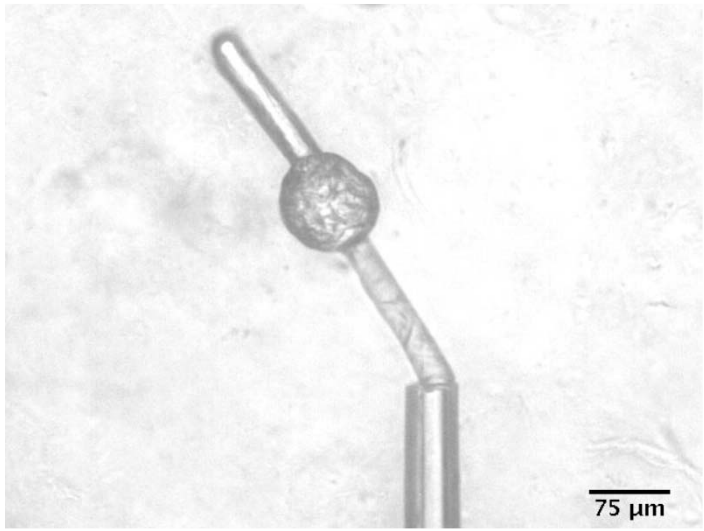

"Dual ball and stick"

Solution and temperature responsive

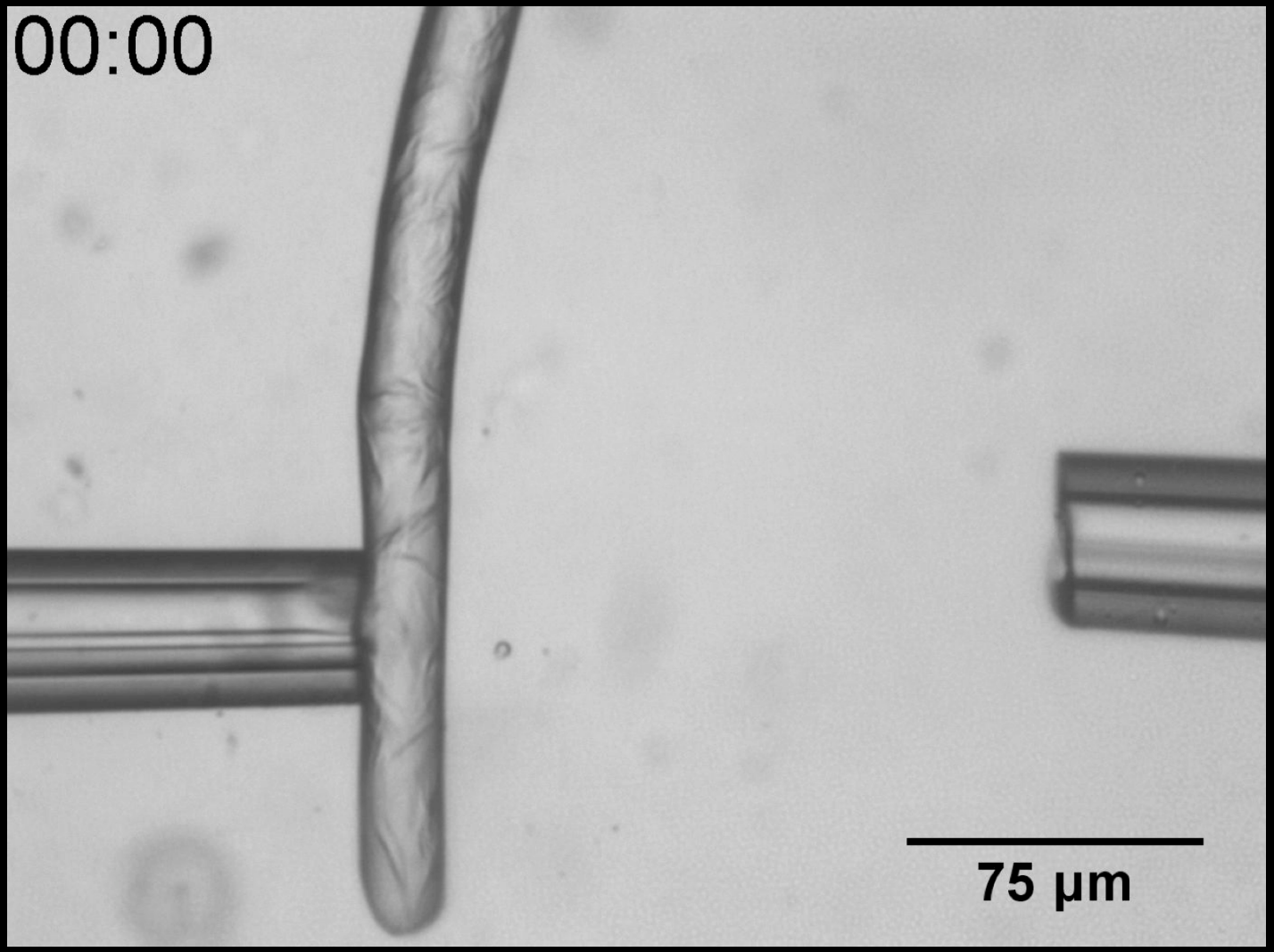

Dilute surfactant to increase surface tension

Caggioni, M., Lenis, J., Bayles, A.V., Furst, E. M. & Spicer, P.T. *Langmuir* 31, 8558–8565 (2015).
Caggioni, M., Bayles, A.V, Lenis, J., Furst, E. M. & Spicer, P.T. *Soft Matter* 10, 7647–7652 (2014).

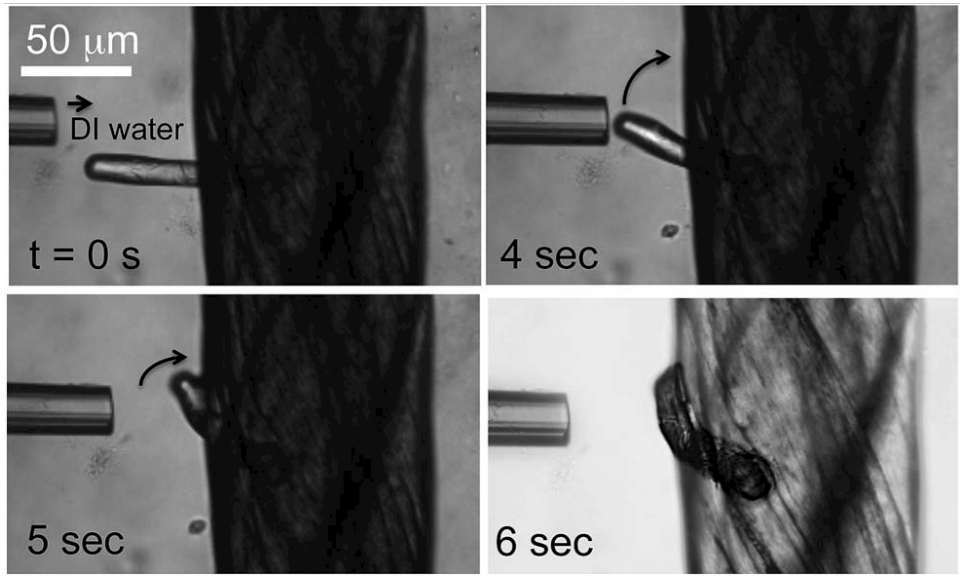

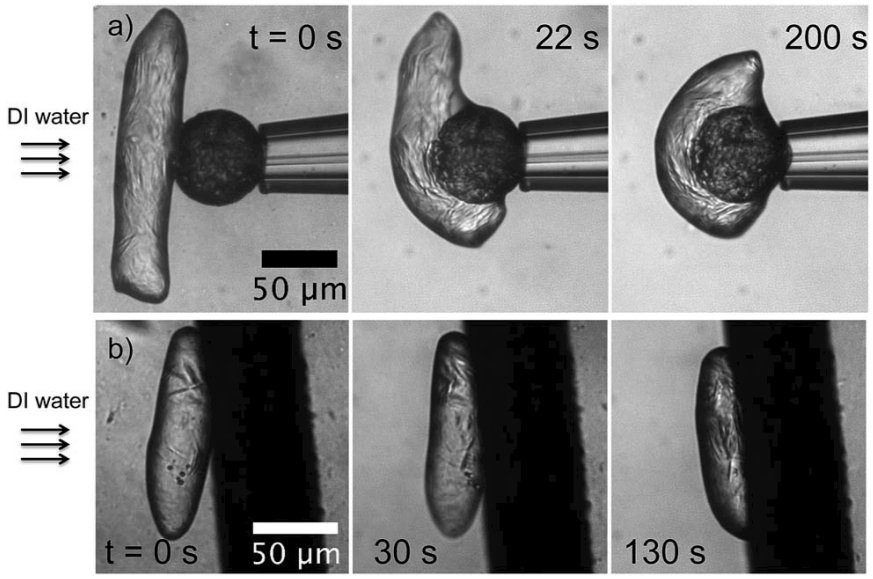

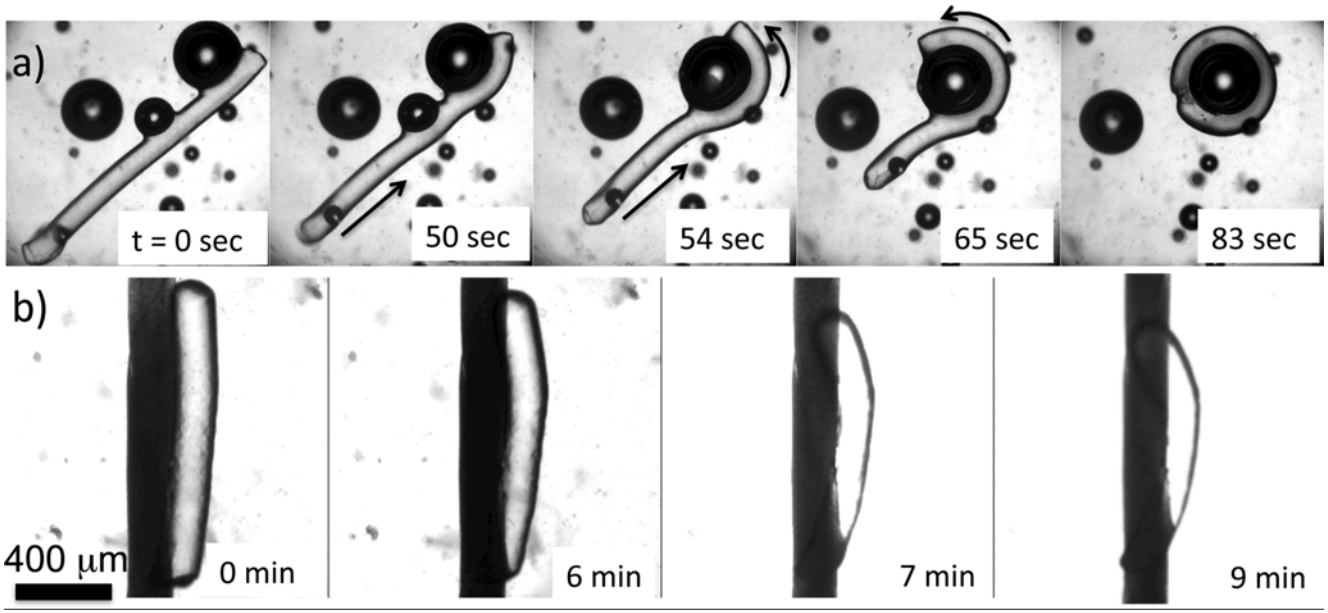

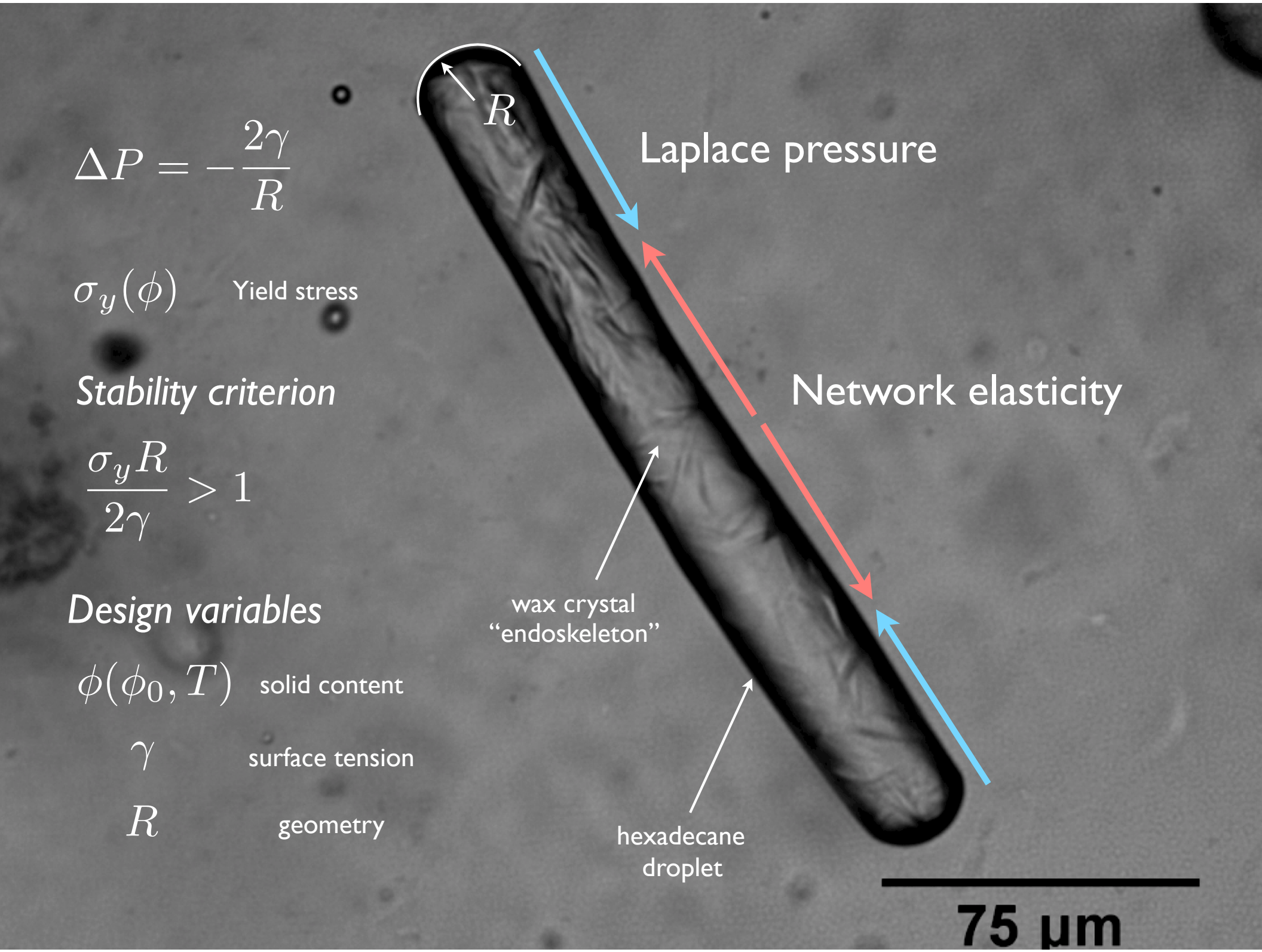
$\Delta P = -\frac{2\gamma}{R}$
$\sigma_y(\phi)$ Yield stress
Stability criterion
$\frac{\sigma_y R}{2\gamma} > 1$
Design variables
$\phi(\phi_0, T)$ solid content
γ surface tension
R geometry
R
Laplace pressure
Network elasticity
wax crystal "endoskeleton"
hexadecane droplet
75 µm

Droplet stability

Caggioni, M., Bayles, A. V, Lenis, J., Furst, E. M. & Spicer, P. T. *Soft Matter* 10, 7647–7652 (2014).

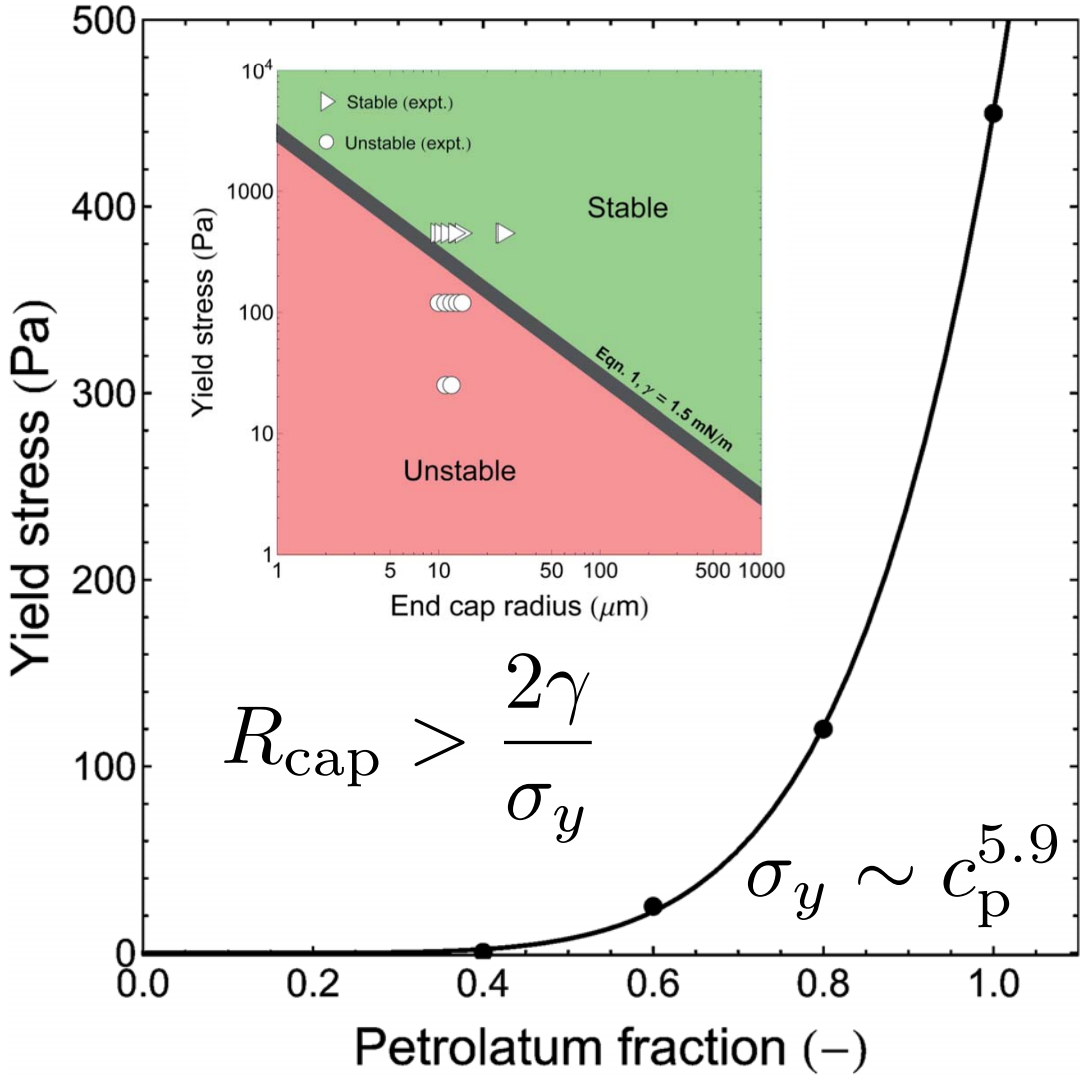

Initially stable droplet

$\gamma = 1.5\,\mathrm{mN\,m^{-1}}$

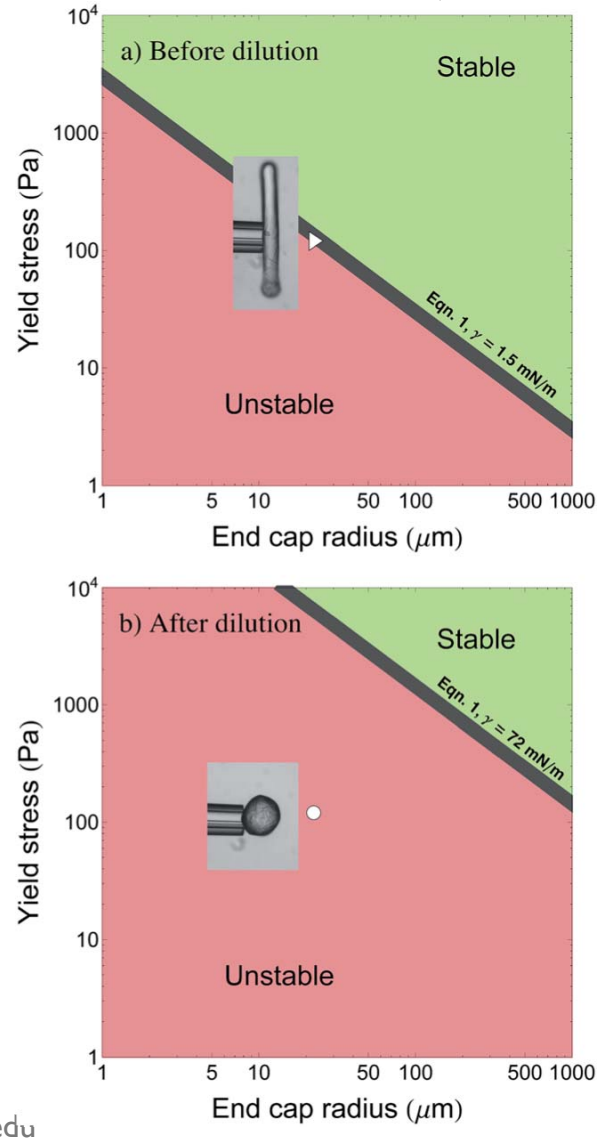

dilution

$\gamma \downarrow$

Shape change

Internal stress in endoskeletal droplet

Arthur P. Boresi and Richard J. Schmidt. *Advanced Mechanics of Materials*. Wiley, New York, 6th edition, 2002.

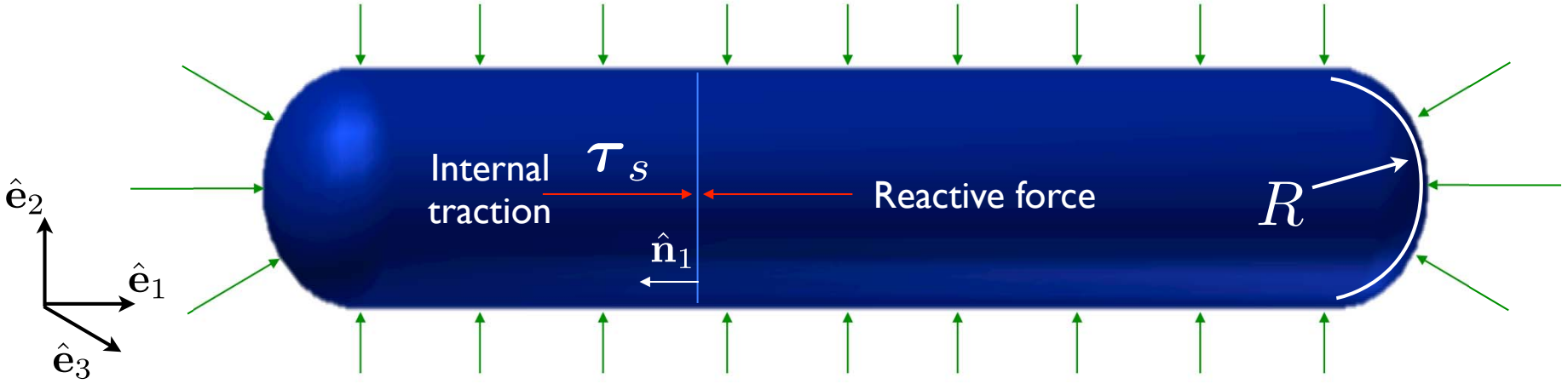

$$\boldsymbol{\tau}_s = \int \mathbf{t} dS$$

$$\mathbf{t}(\mathbf{r}) = \gamma H(\mathbf{r}) \hat{\mathbf{n}}$$

surface traction vector

$$H(\mathbf{r}) = \frac{1}{2}\left(\frac{1}{R_1} + \frac{1}{R_2}\right)$$

Mean Gaussian curvature

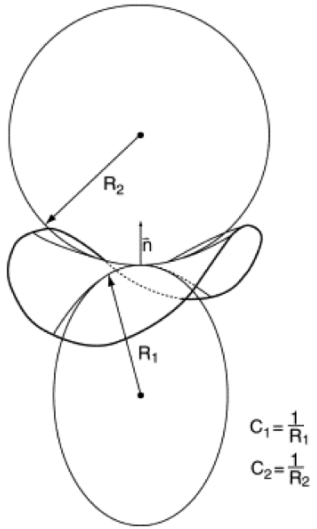

Decompose stress tensor to principal stresses

$$\boldsymbol{\tau} \cdot \hat{\mathbf{n}} = \begin{bmatrix} \sigma_{xx} & \tau_{xy} & \tau_{xz} \\ \tau_{yx} & \sigma_{yy} & \tau_{yz} \\ \tau_{zx} & \tau_{zy} & \sigma_{zz} \end{bmatrix} \rightarrow \begin{bmatrix} \sigma_1 & 0 & 0 \\ 0 & \sigma_2 & 0 \\ 0 & 0 & \sigma_3 \end{bmatrix}$$

von Mises yield criterion $\sigma_{vM} > \sigma_y$

$$\sigma_{\mathrm{vM}} = \sqrt{\frac{(\sigma_1 - \sigma_2)^2 + (\sigma_1 - \sigma_3)^2 + (\sigma_3 - \sigma_2)^2}{2}}$$

Spherocylinder internal stress distribution

Alexandra V. Bayles, Tamás Prileszky, P. J. Spicer and E. M. Furst, *Langmuir*, 34, 4116–4121 (2018).

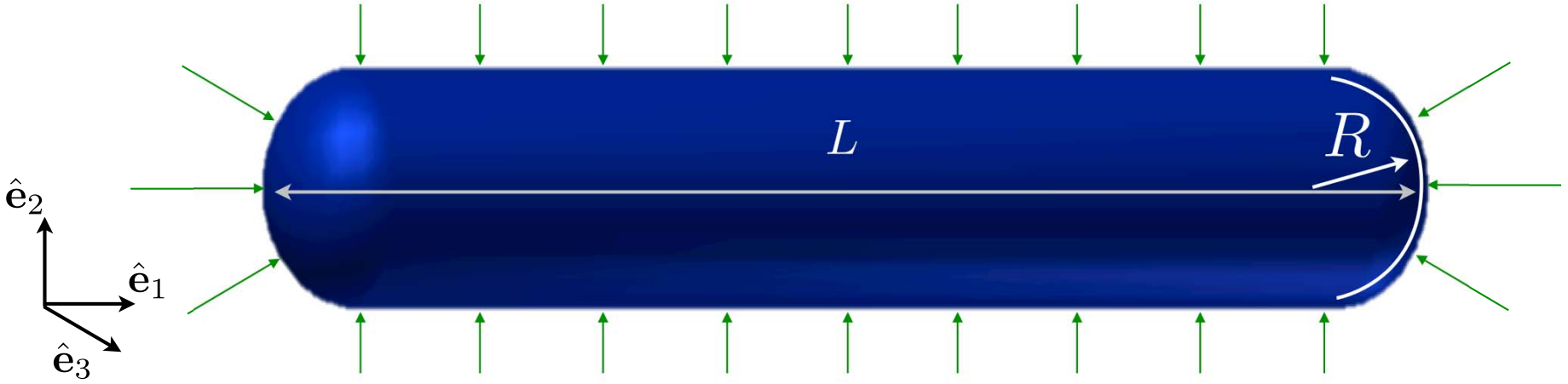

Ends

$$\sigma_2 = \frac{2\gamma}{R}$$

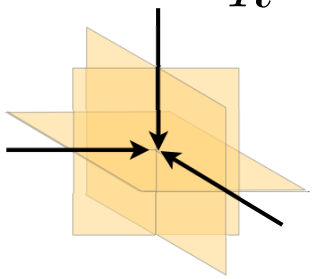

$$\sigma_1 = \frac{2\gamma}{R}$$

$$\sigma_3 = \frac{2\gamma}{R}$$

$$\sigma_{\mathrm{vM}} = \sqrt{\frac{(\sigma_1-\sigma_2)^2+(\sigma_1-\sigma_3)^2+(\sigma_3-\sigma_2)^2}{2}}$$

$$\sigma_{vM} = 0$$

Rod section

$$\sigma_2 = \frac{\gamma}{R}$$

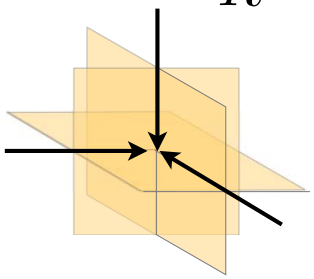

$$\sigma_1 = \frac{2\gamma}{R}$$

$$\sigma_3 = \frac{\gamma}{R}$$

$$\sigma_{vM} = \frac{1}{\sqrt{2}}\left(\frac{\gamma}{R}\right)$$

Spherocylinder internal stress distribution

Alexandra V. Bayles, Tamás Prileszky, P. J. Spicer and E. M. Furst, *Langmuir*, 34, 4116–4121 (2018).

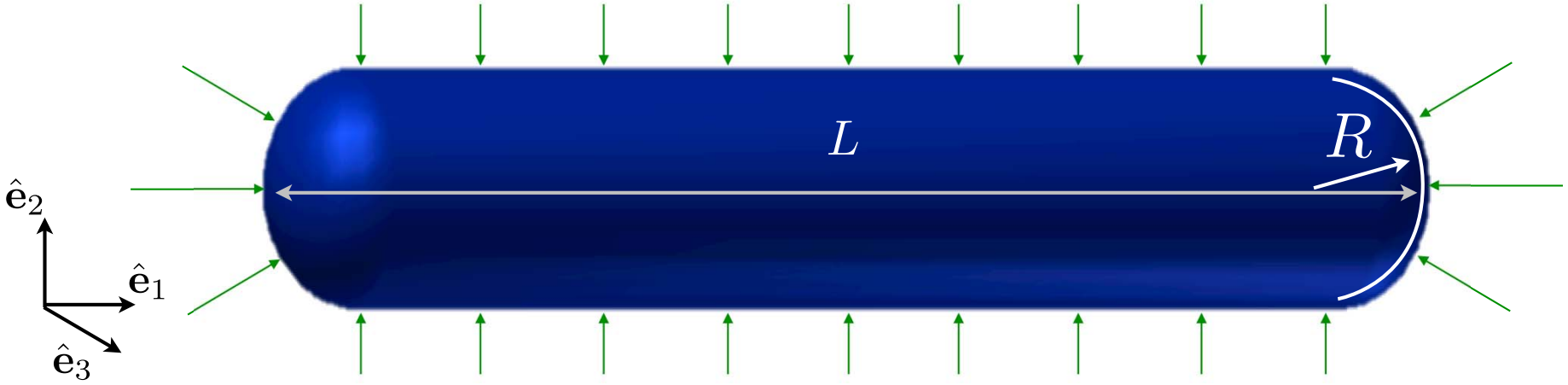

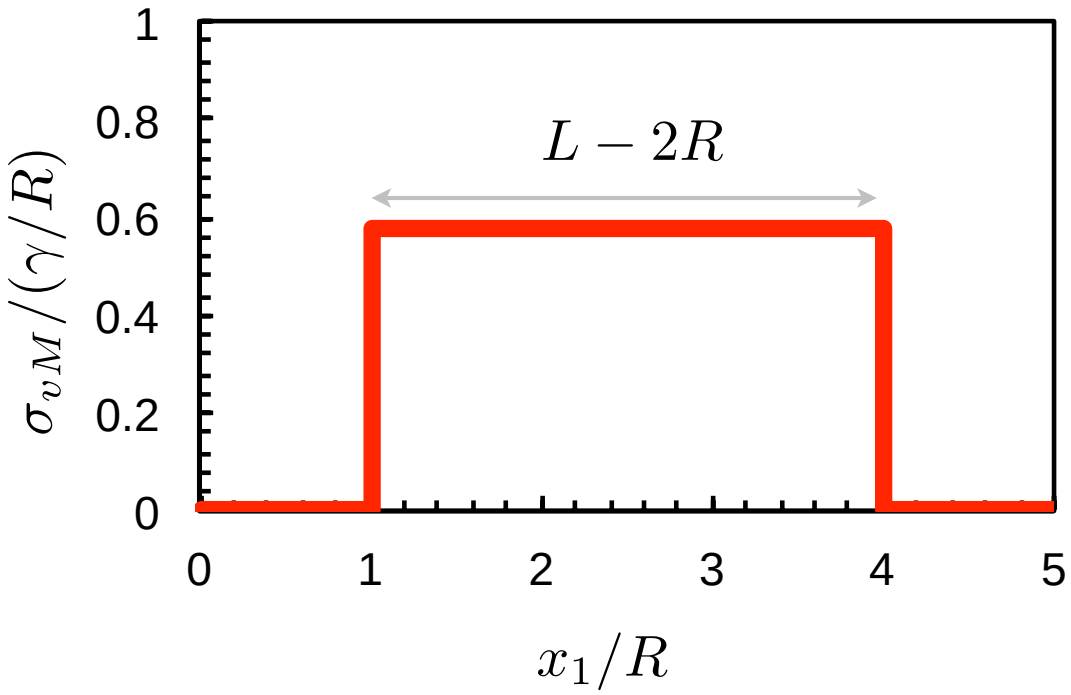

Ball-and-stick internal stress distribution

Alexandra V. Bayles, Tamás Prileszky, P. J. Spicer and E. M. Furst, *Langmuir*, 34, 4116–4121 (2018).

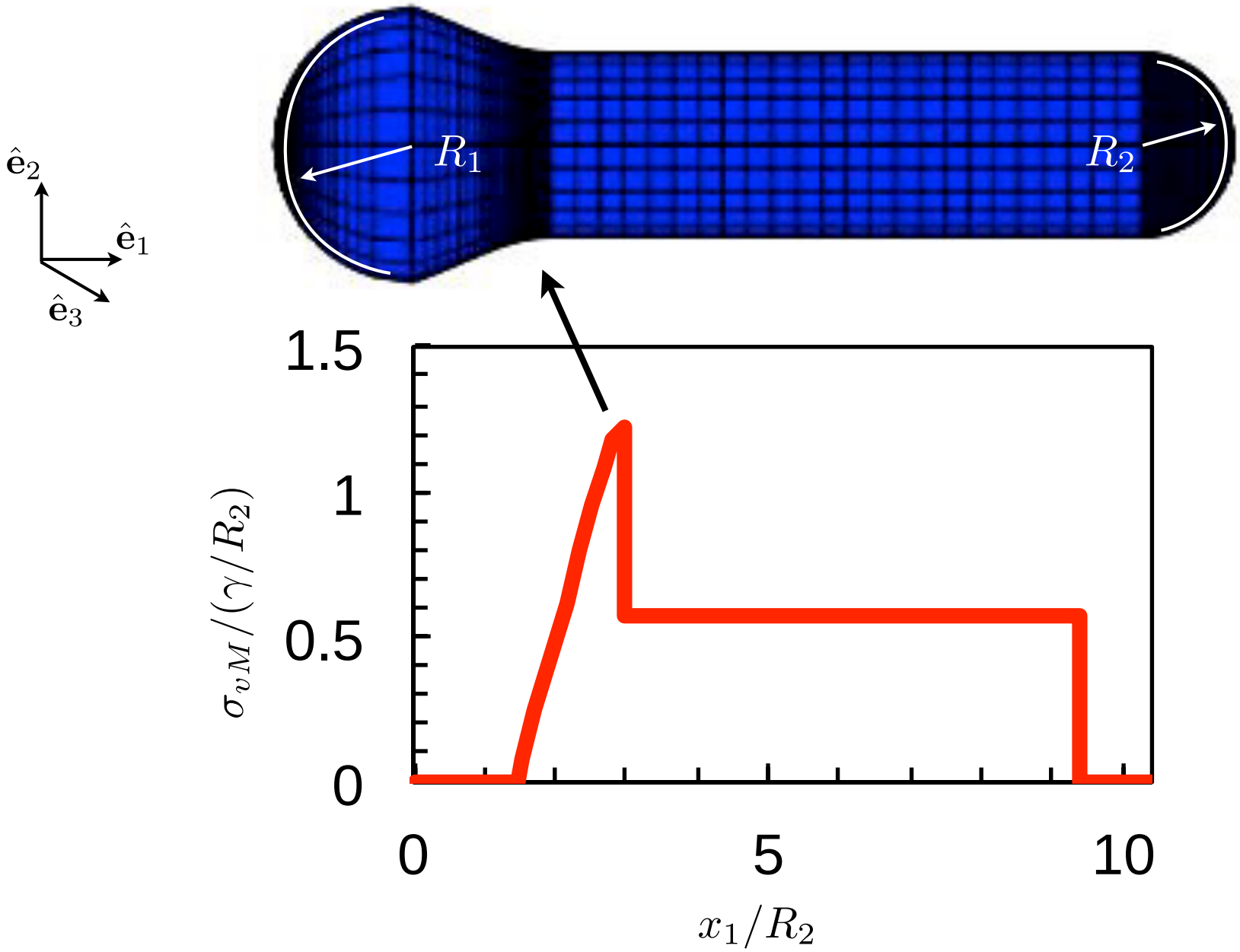

Programmed reconfiguration by shape

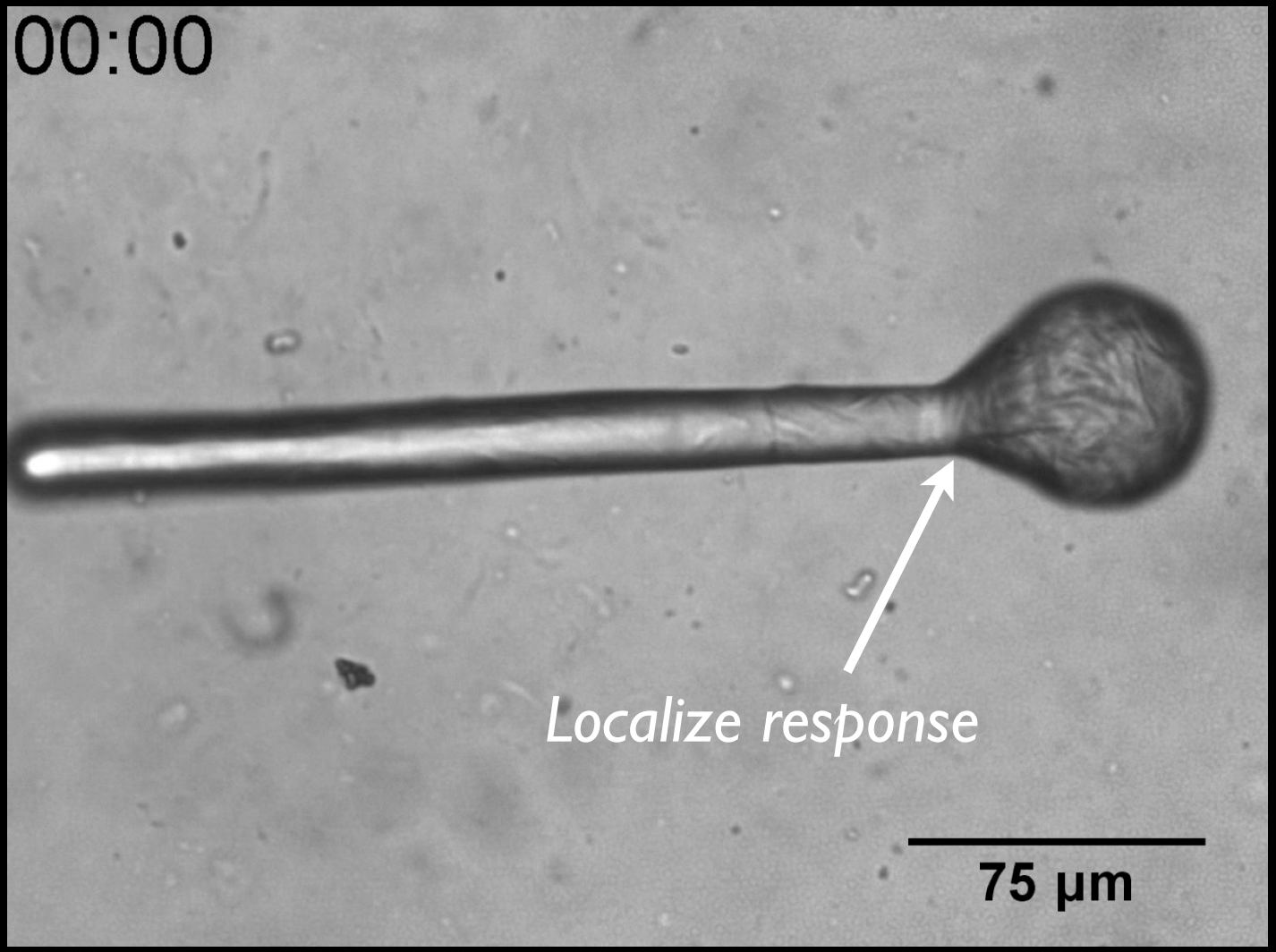

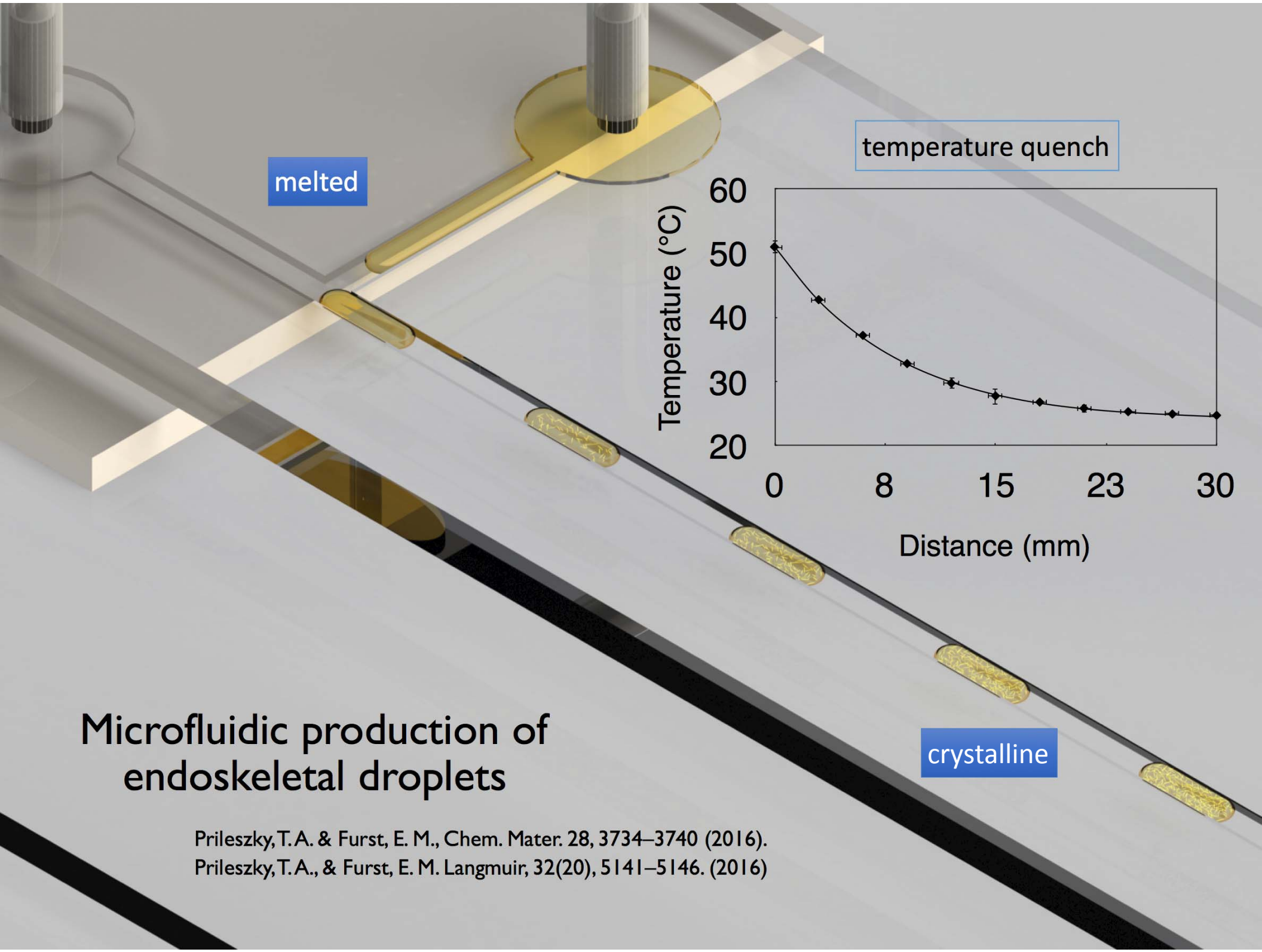

Microfluidic production of endoskeletal droplets

Prileszky, T. A. & Furst, E. M., Chem. Mater. 28, 3734–3740 (2016).
Prileszky, T. A., & Furst, E. M. Langmuir, 32(20), 5141–5146. (2016)

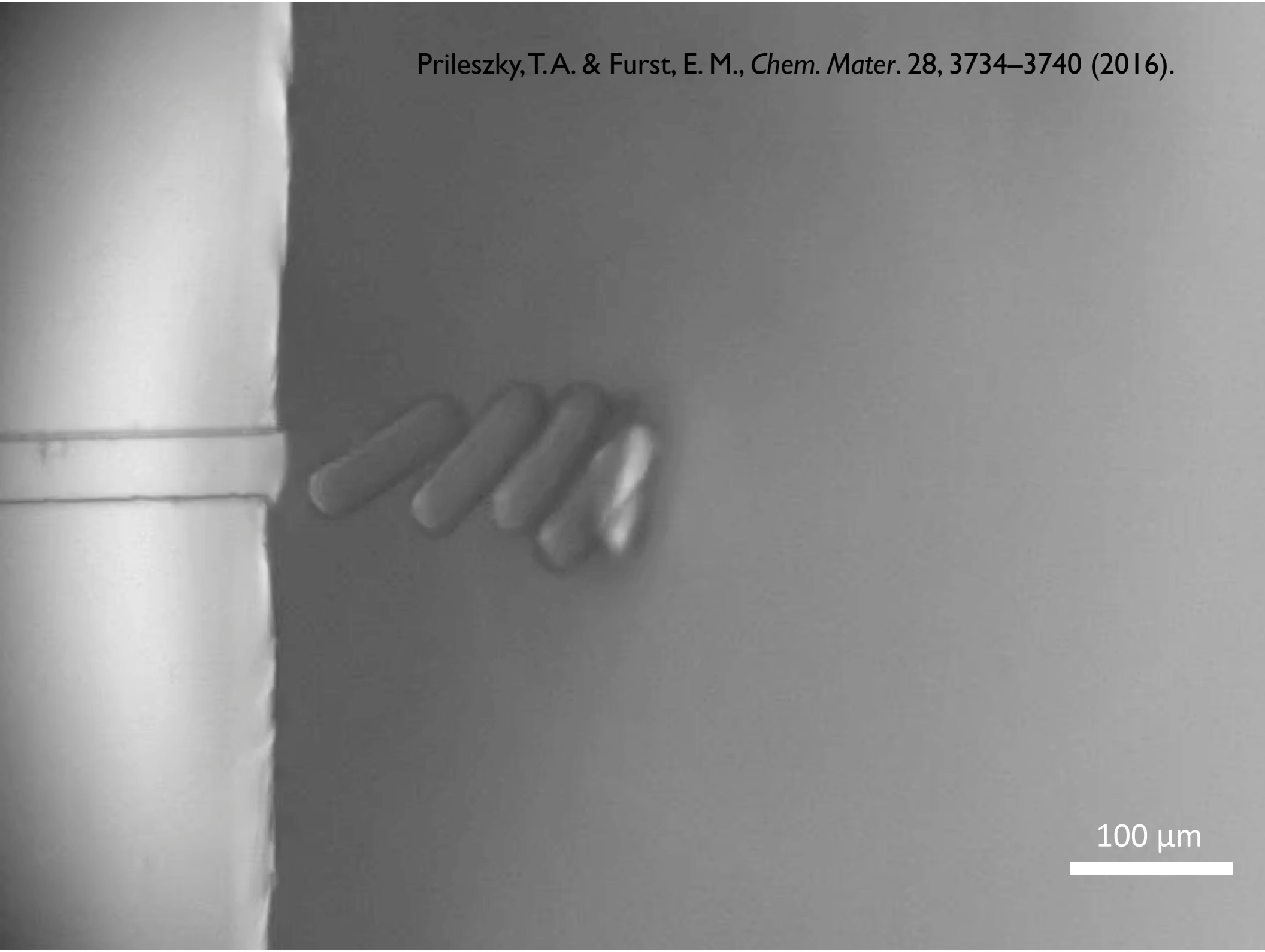
Prileszky, T. A. & Furst, E. M., *Chem. Mater.* 28, 3734–3740 (2016).
100 µm

Microfluidic production of endoskeletal droplets

Prileszky, T. A. & Furst, E. M., *Chem. Mater.* 28, 3734–3740 (2016).
Prileszky, T. A., & Furst, E. M. *Langmuir*, *32*(20), 5141–5146. (2016)

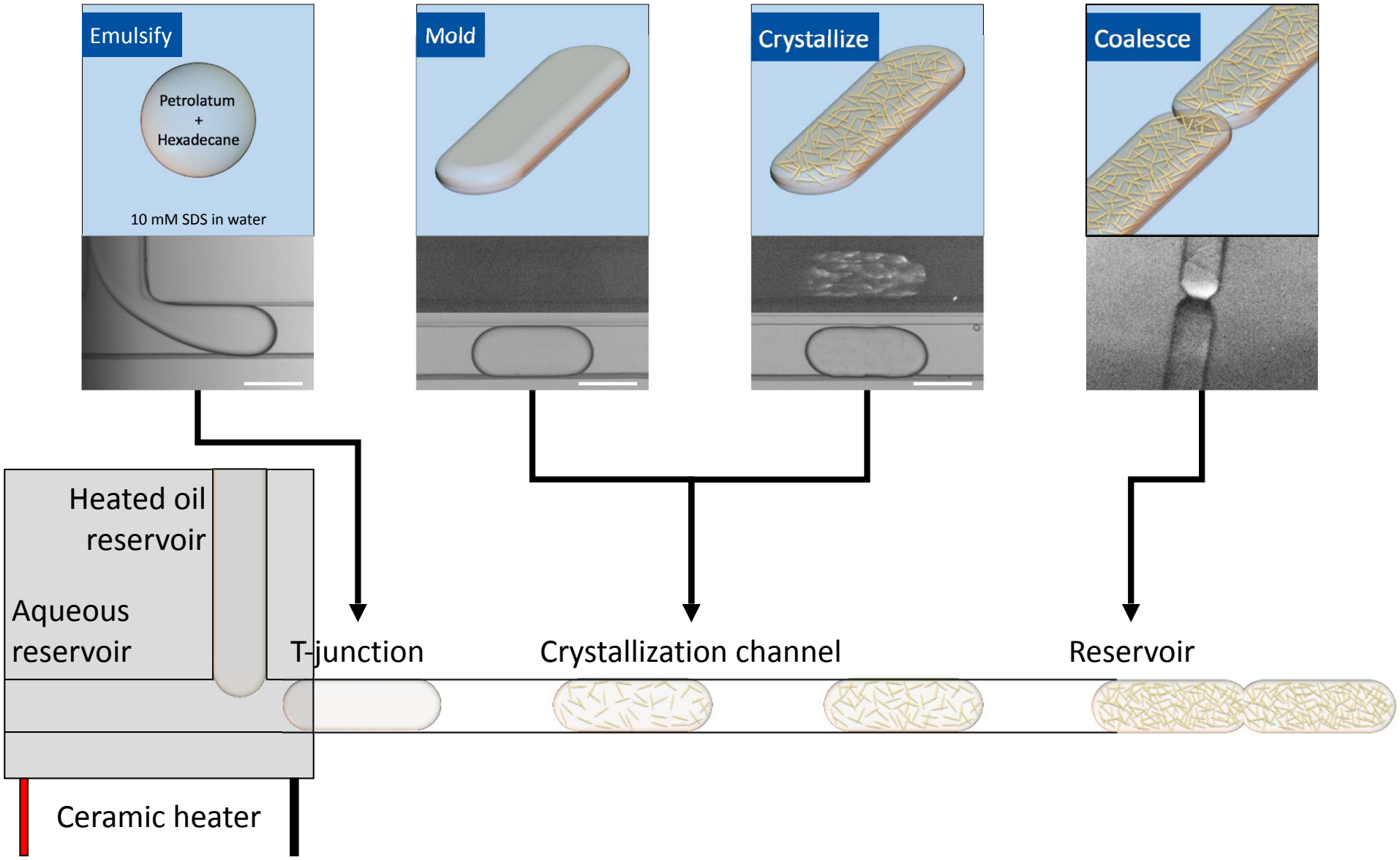

Droplet polarization

Prileszky, T. A., & Furst, E. M. Langmuir, 32(20), 5141–5146. (2016)

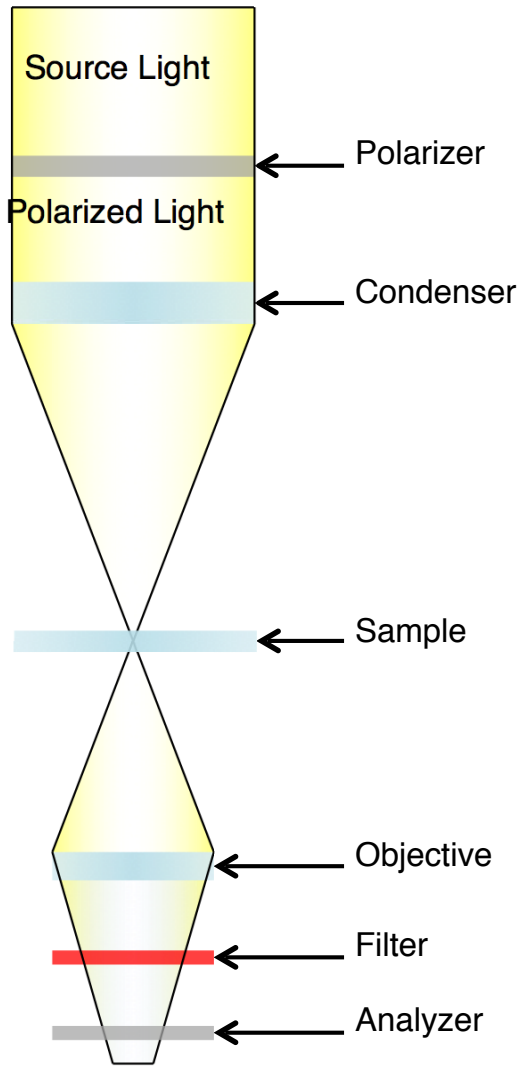

$I_{\perp}$

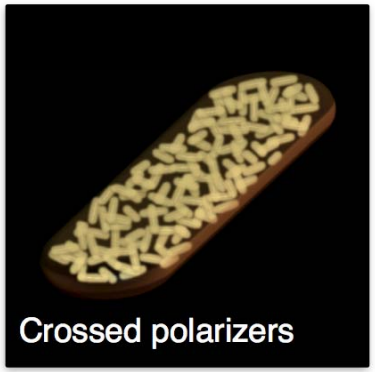

$I_{\parallel}$

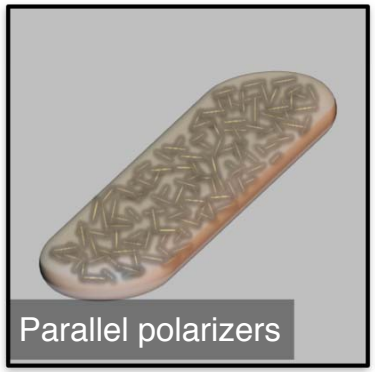

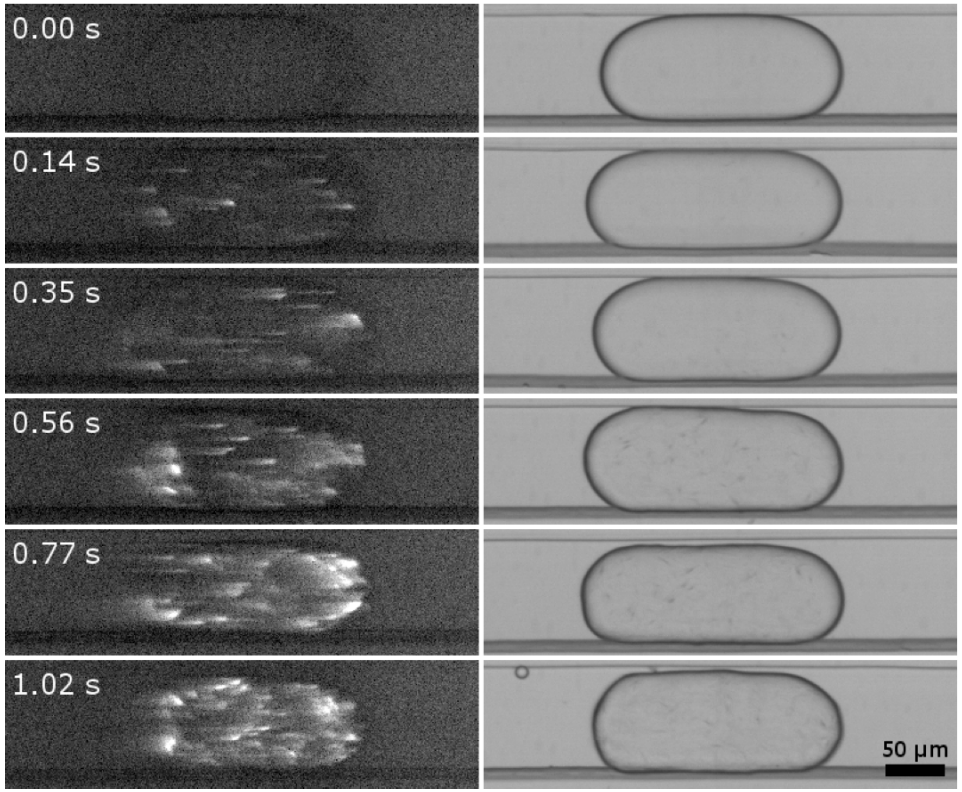

Depolarization ratio and crystallite orientation

Prileszky, T. A., & Furst, E. M. *Langmuir*, 32(20), 5141–5146. (2016)

$$J = \frac{2I_{\perp}}{I_{\perp} + I_{\parallel}} = 1 - e^{-D \cdot E \cdot S}$$

Ziabicki, A. *J. Opt. A Pure Appl. Opt.* 7, 774 (2005).
Ziabicki, A. & Misztal-Faraj, B. *Mater. Sci.* 24, 493 (2006).

$D(\lambda)$ Average optical retardation of a birefringent plate

$E(n)$ Average number of birefringent plates

$S(\phi)$ Average plate orientation

$$S = \frac{\ln\left(1 - J(\lambda, 45°)\right)}{\ln\left(1 - J(\lambda, 45°)\right) + \ln\left(1 - J(\lambda, 0°)\right)}$$

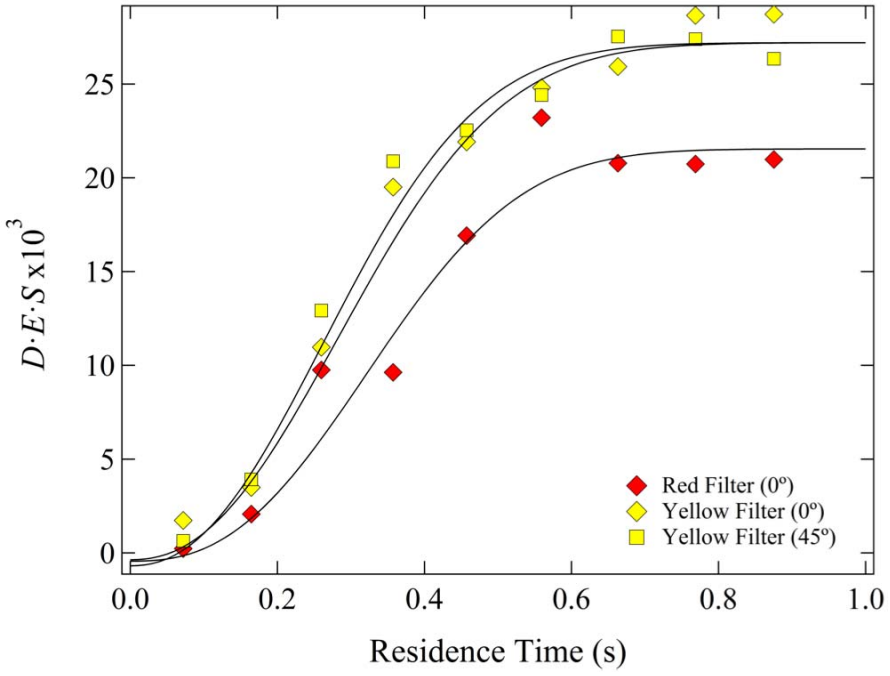

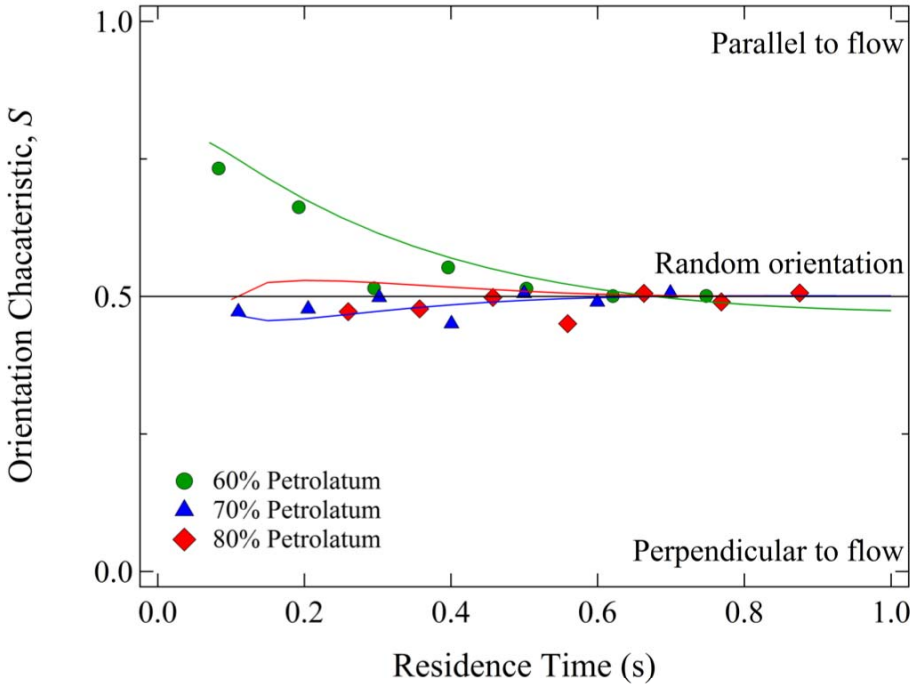

Degree of crystallinity

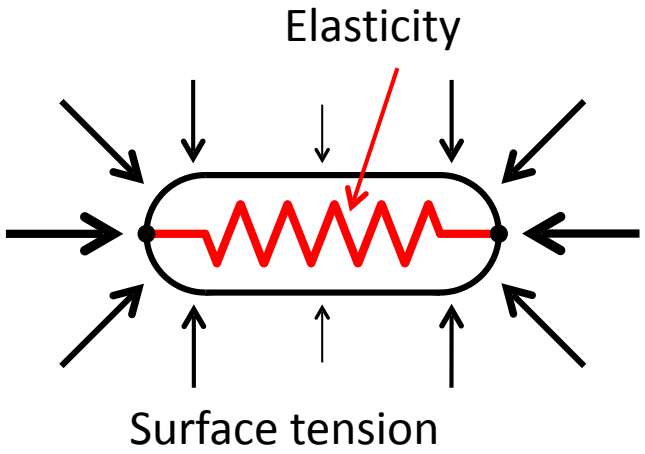

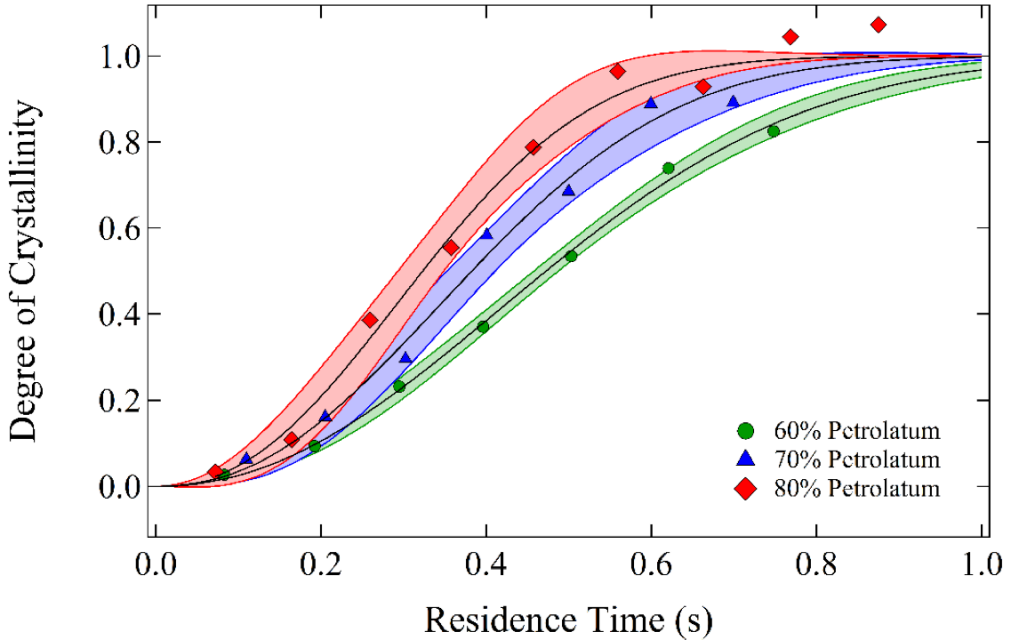

Prileszky, T. A., & Furst, E. M. *Langmuir*, *32*(20), 5141–5146. (2016)

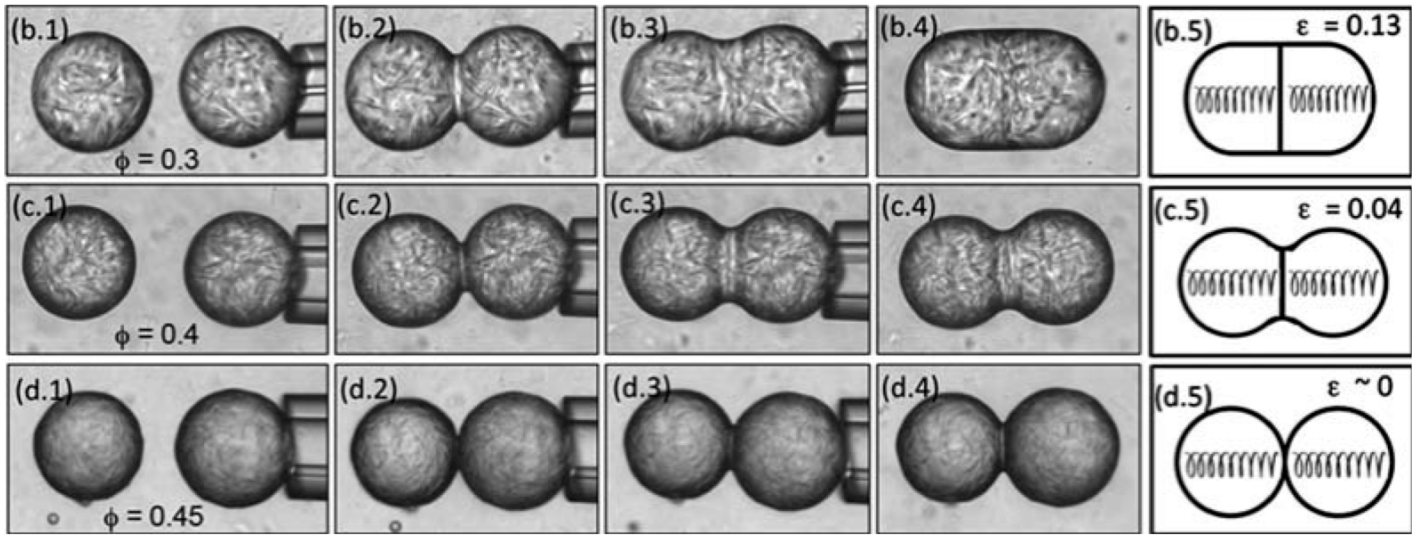

Pawar, A. B., *et al. Faraday Discussions*, *158*, 341. (2012)

Supra-structure droplet assembly

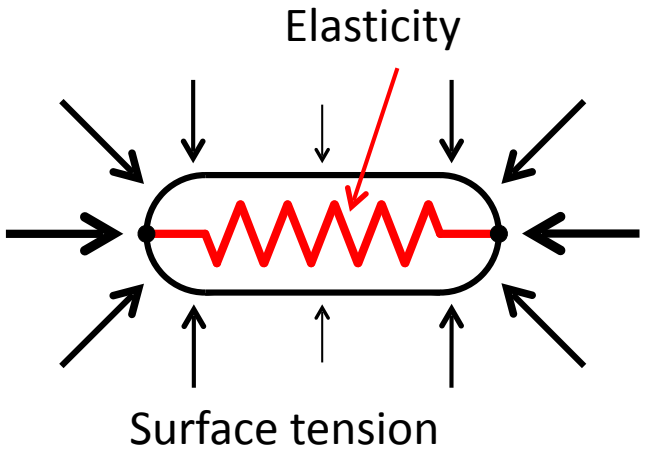

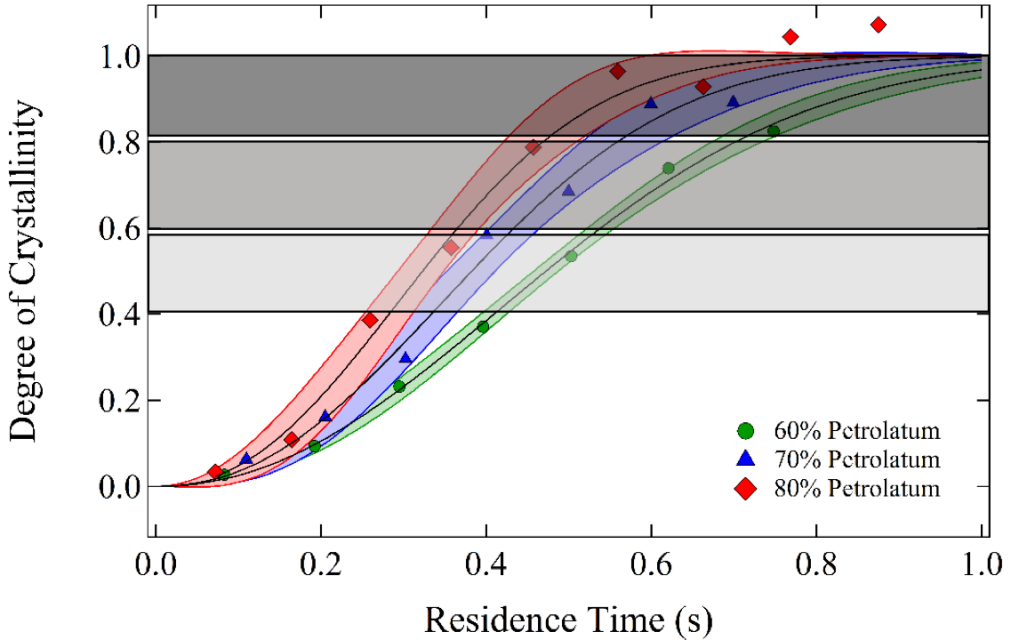

Prileszky, T. A., & Furst, E. M. *Langmuir*, *32*(20), 5141–5146. (2016)

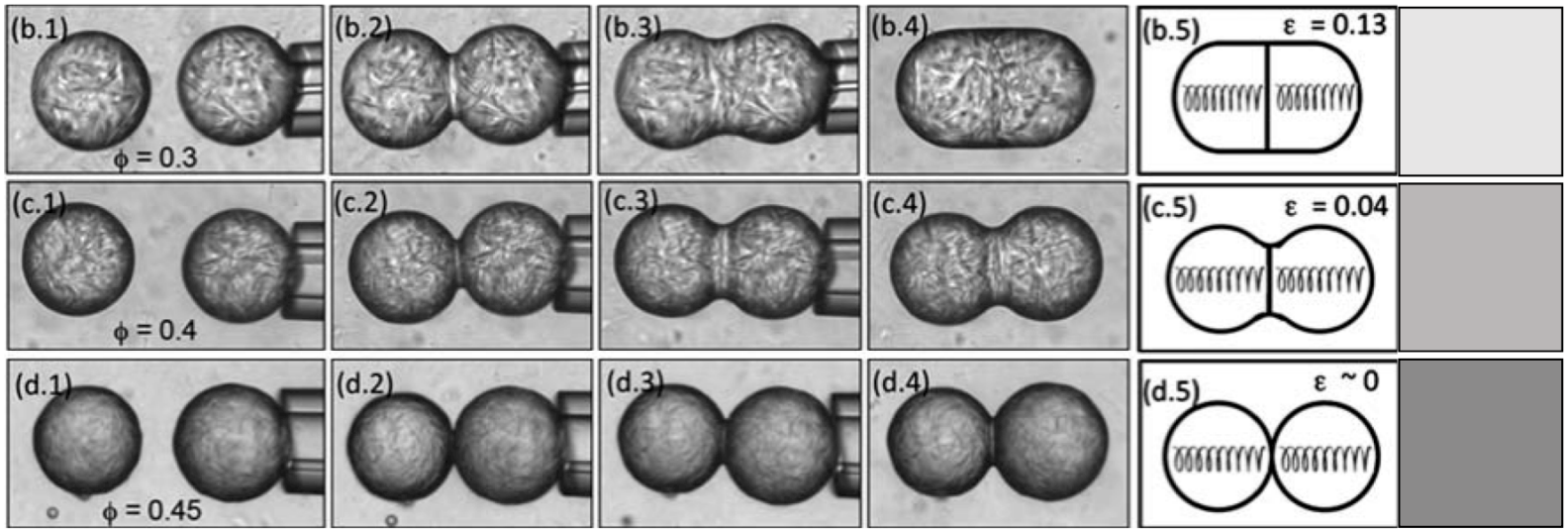

Pawar, A. B., *et al. Faraday Discussions*, *158*, 341. (2012)

Supra-structure droplet assembly

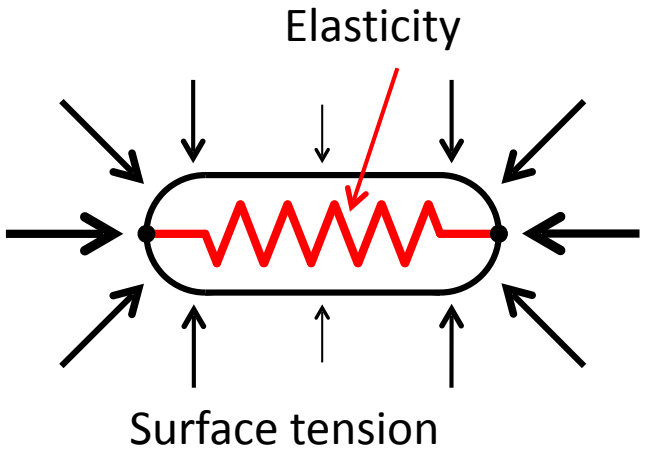

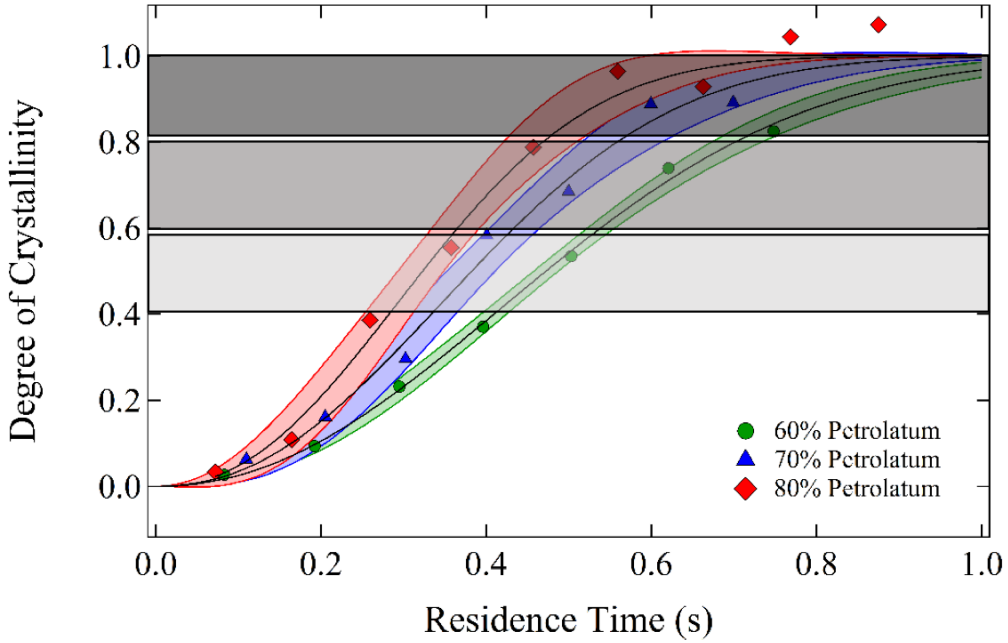

Prileszky, T. A., & Furst, E. M. *Langmuir*, *32*(20), 5141–5146. (2016)

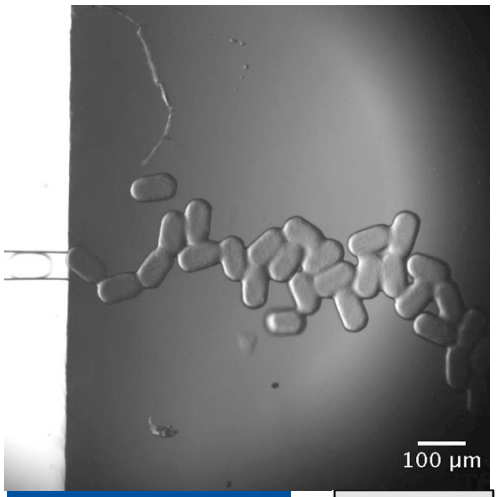

Herringbones
Lower crystallinity

Prileszky, T. A. & Furst, E. M., *Chem. Mater.* 28, 3734–3740 (2016).

Magnetically responsive droplets

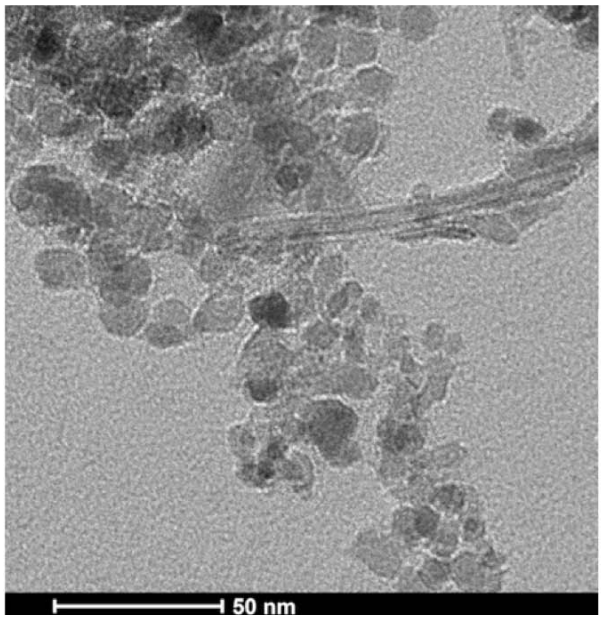

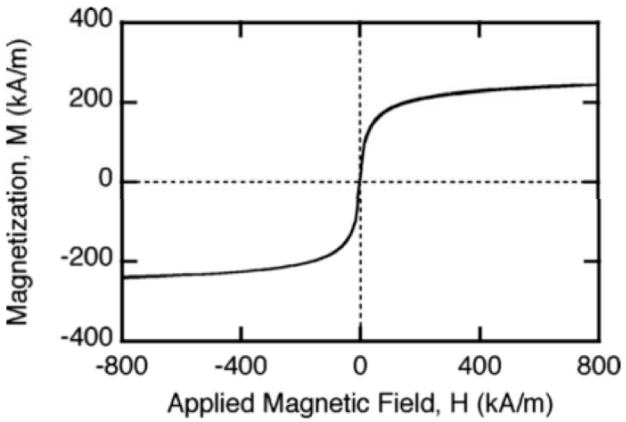

Super-paramagnetic
iron oxide nanoparticles

Bee, A., Massart, R. & Neveu, S., J. Magn. Magn. Mat. 149, 6–9 (1995).

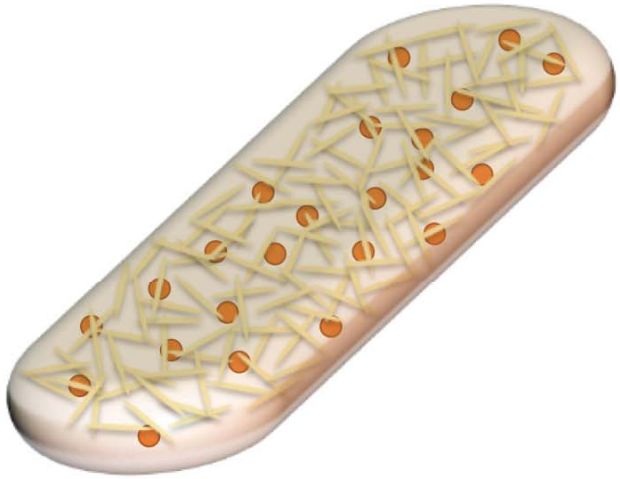

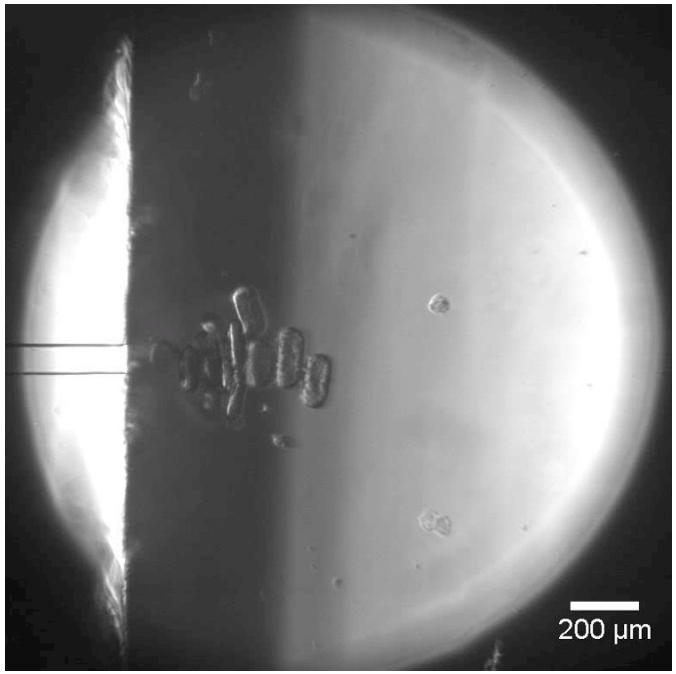

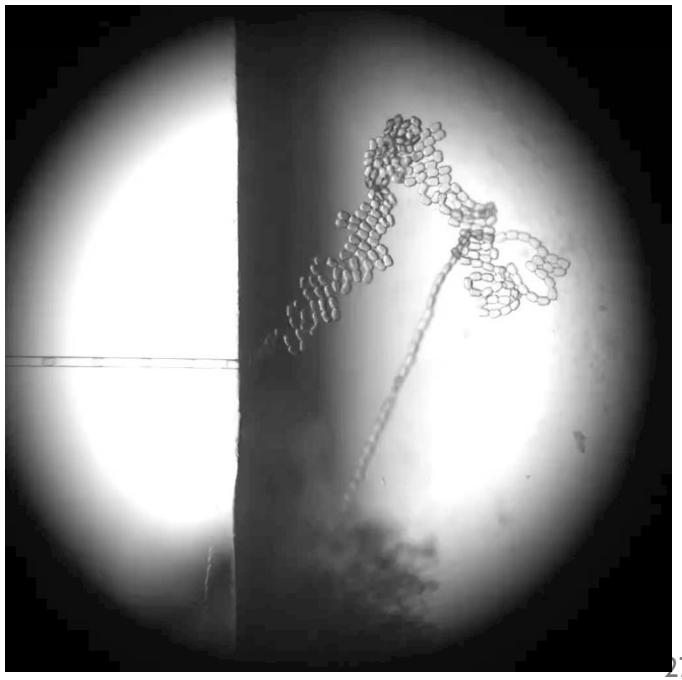

Alignment, magnetophoresis

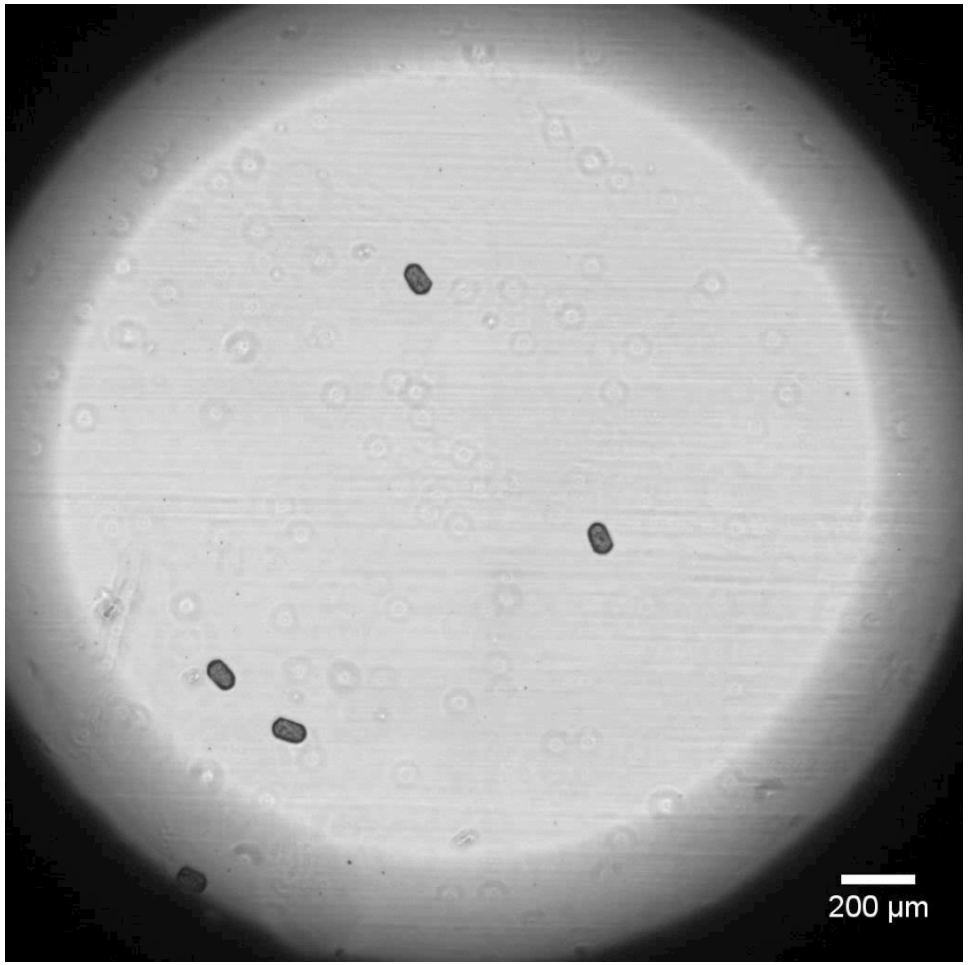

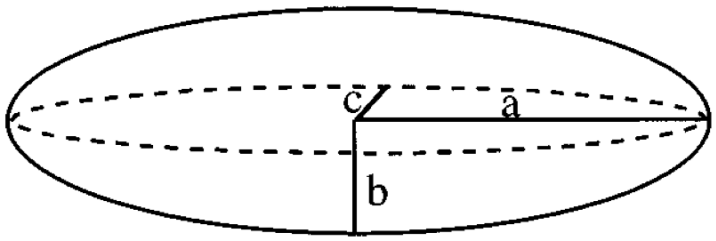

$$\mathbf{m}_h = \mu_0 V_a \left[\frac{\chi_a \mathbf{H}}{1 + (4\pi\chi_a) n_z} \right]$$

$\mathbf{m}_h$ = magnetic moment
n_z = demagnetizing factor

$$n_z = \left[\frac{1 - e^2}{2e^3} \right] \left[\ln\left(\frac{1+e}{1-e} \right) - 2e \right]$$

$$e = \left(1 - \frac{b^2}{a^2} \right)^{\frac{1}{2}}$$

$$\mathbf{T} = \mathbf{m} \cdot \mathbf{B}$$

$$\mathbf{F} = \mathbf{m} \cdot \nabla \mathbf{B}$$

Droplet chaining by induced magnetic interactions

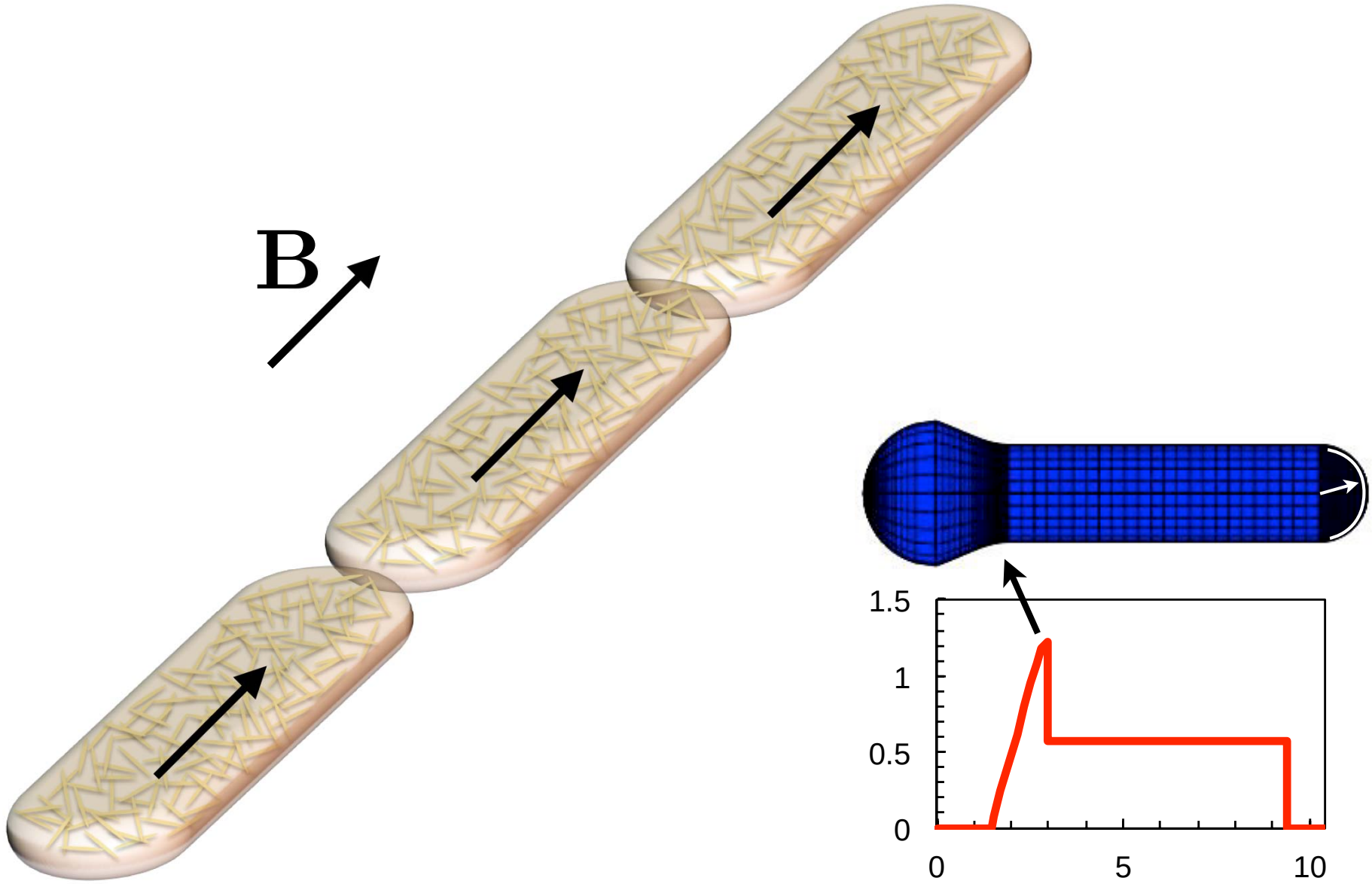

Build foldable droplet units
"Droplet origami"

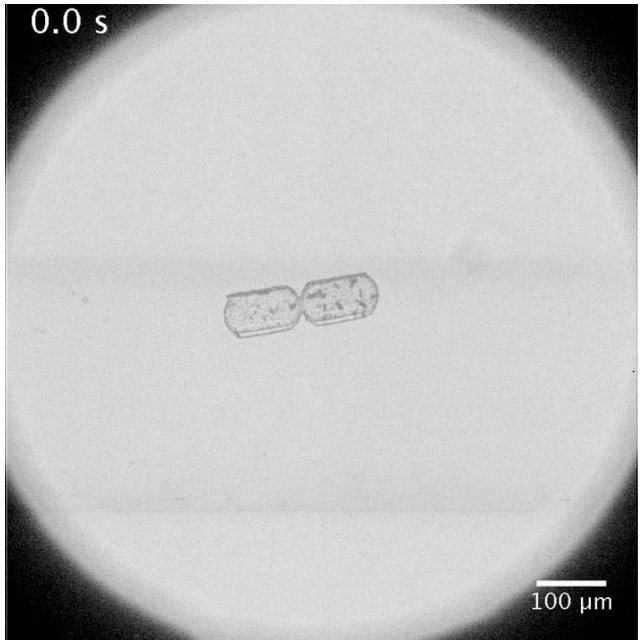

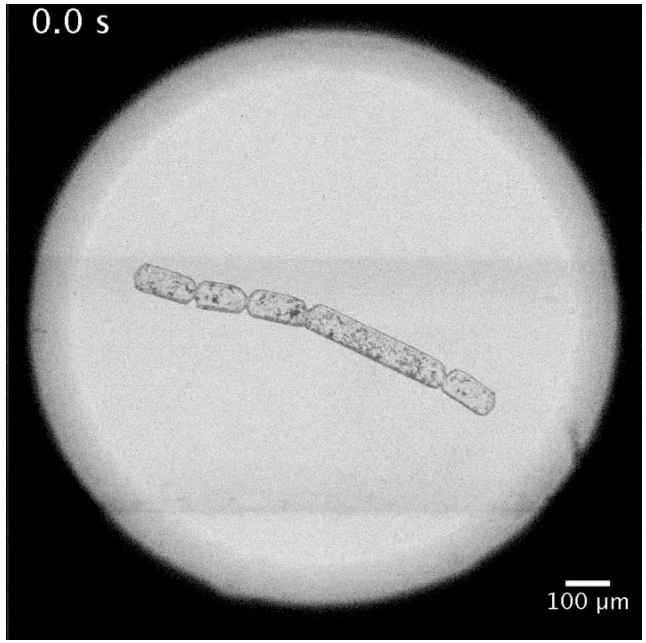

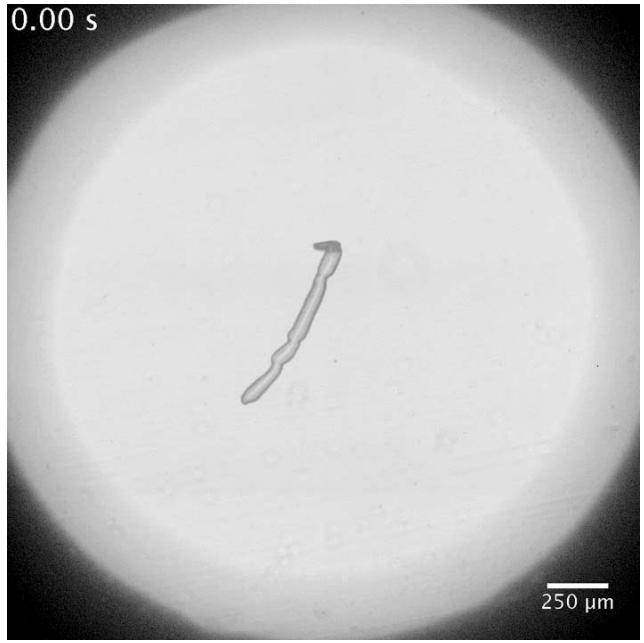

Advantages of shape anisotropy for deposition

Delivery / transport

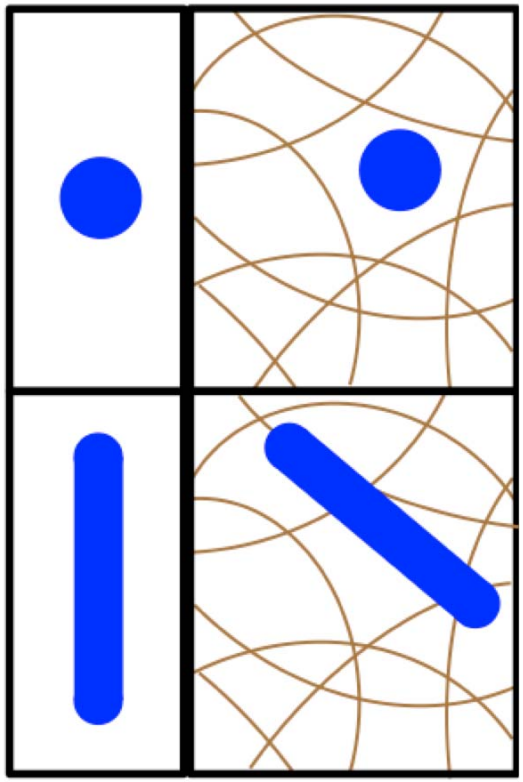

better filtration, higher collision cross-section

Retention

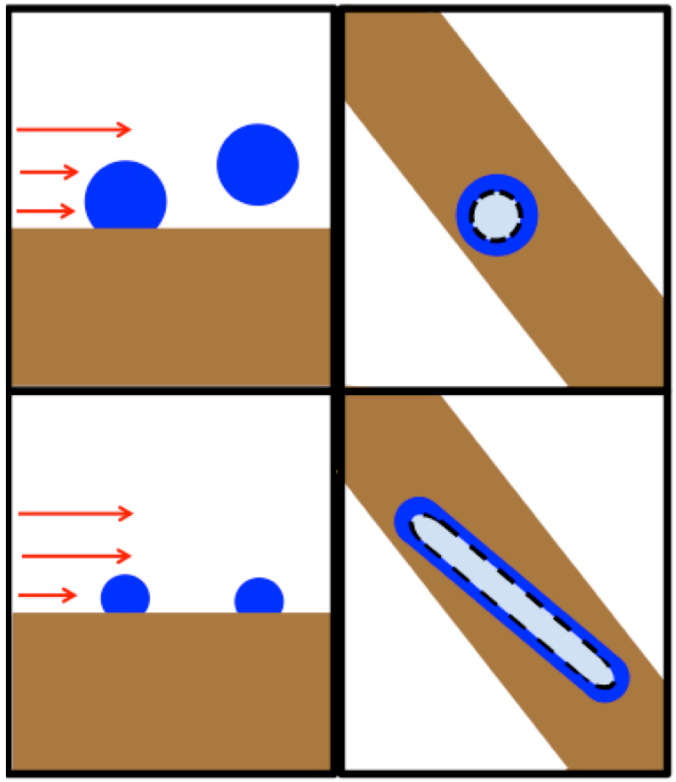

greater contact, adhesion, shape reconfiguration

Spicer et al. U.S. Patent No. 9,597,648 B2

Reconfigurable delivery vehicle

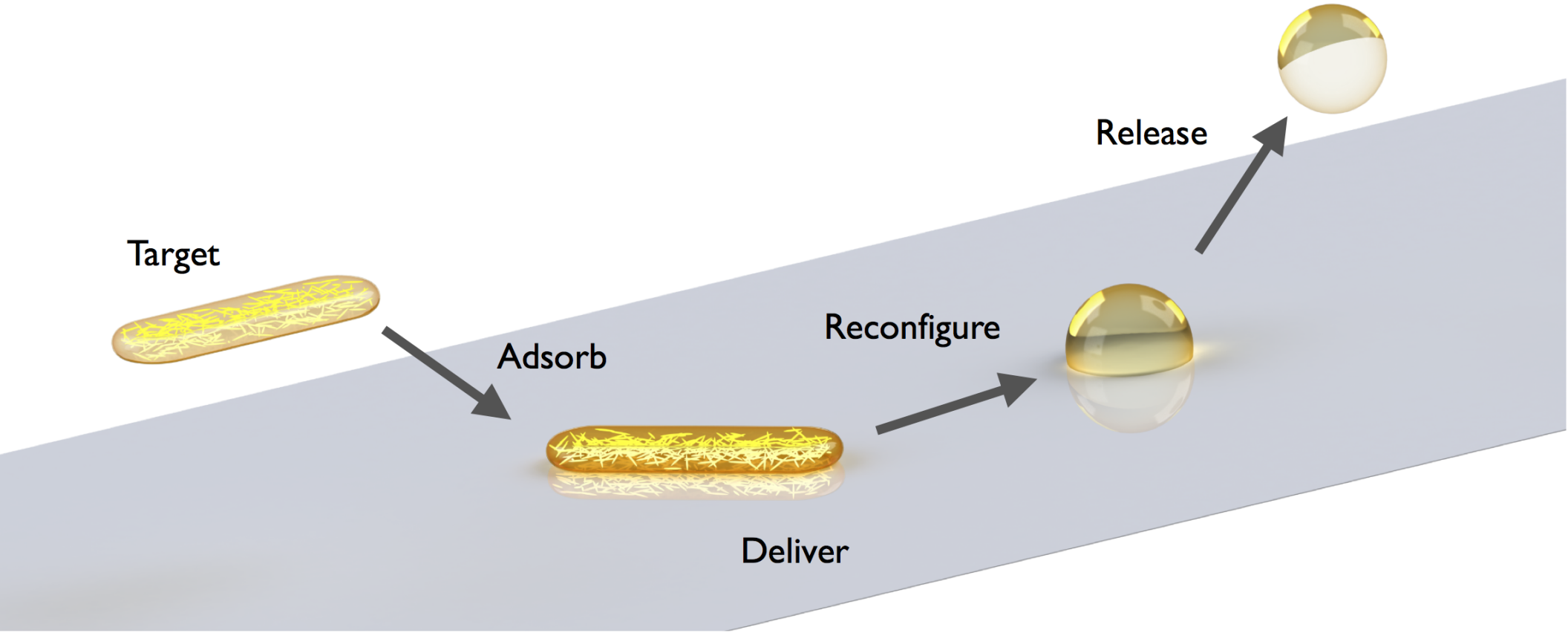

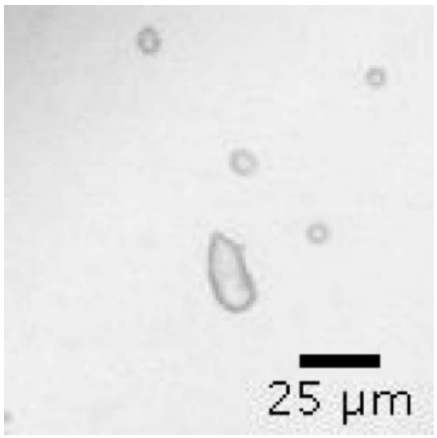

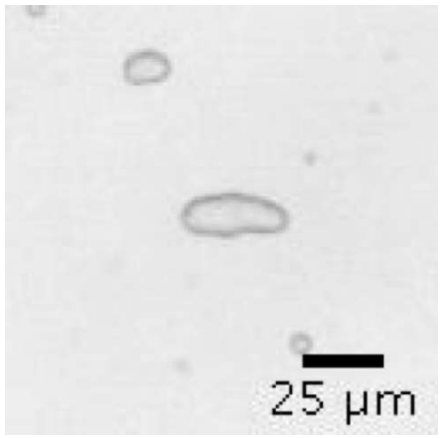

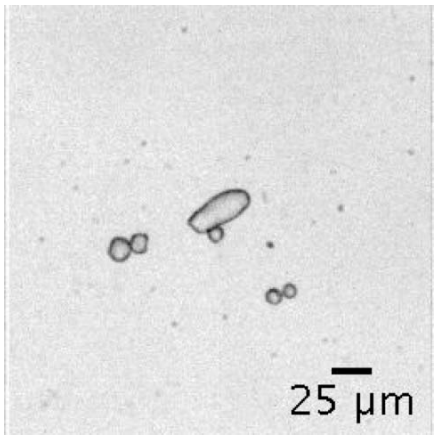

Deposition

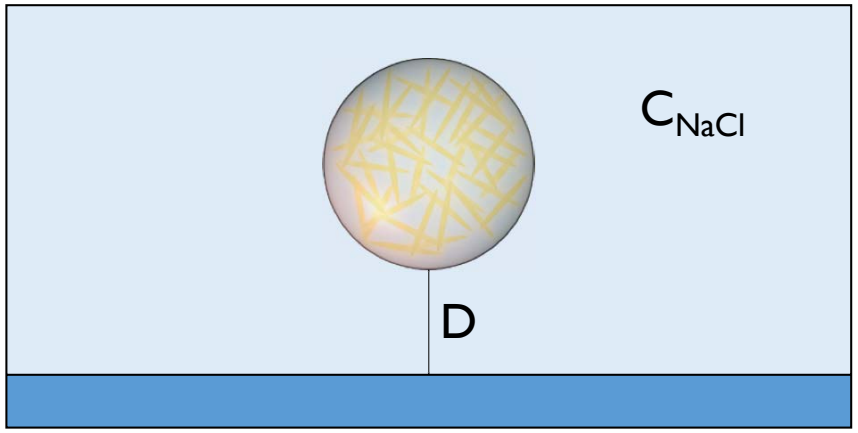
C_{NaCl}
D

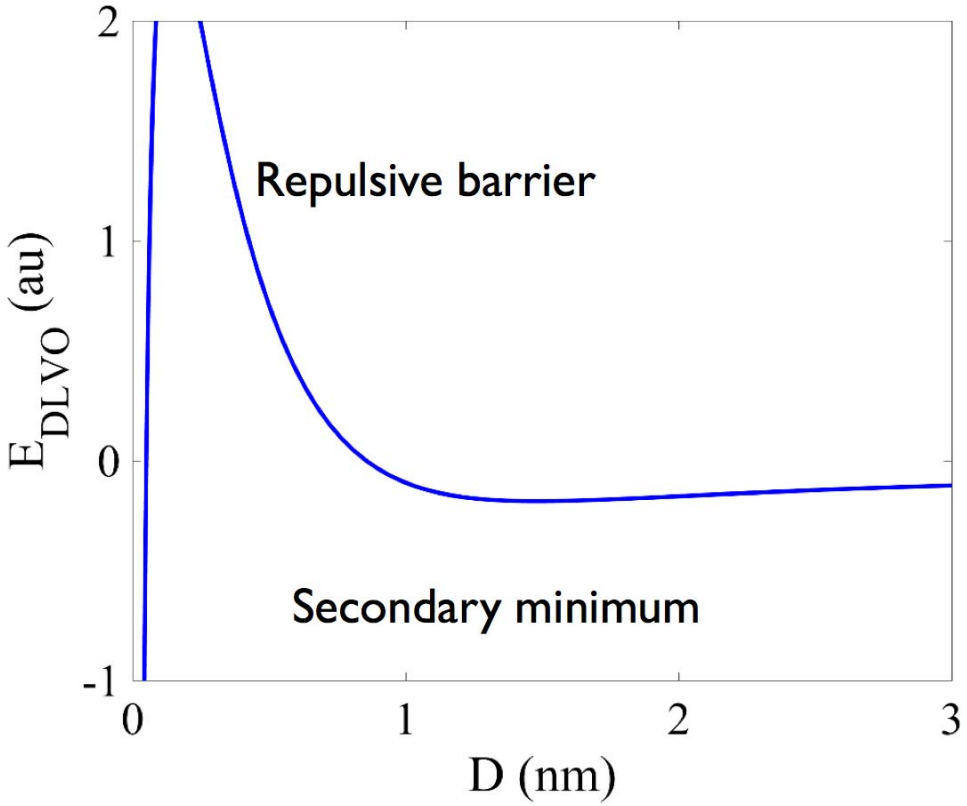
Repulsive barrier
Secondary minimum
E_{DLVO} (au)
D (nm)
2
1
0
-1
0
1
2
3

Depositi

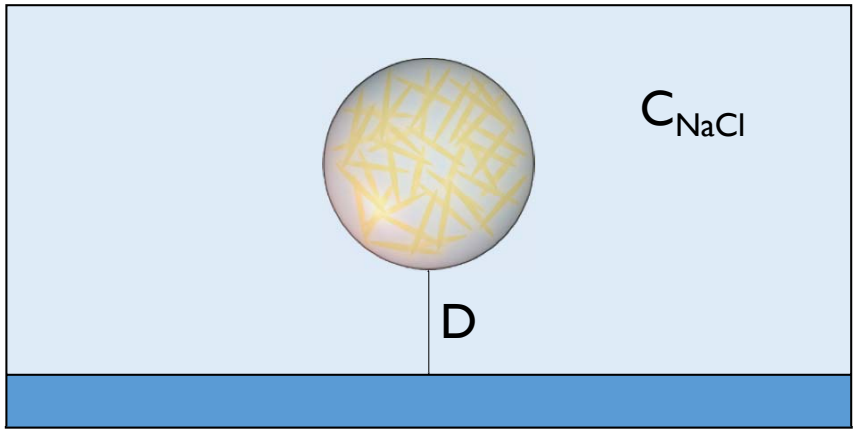
C_{NaCl}
D

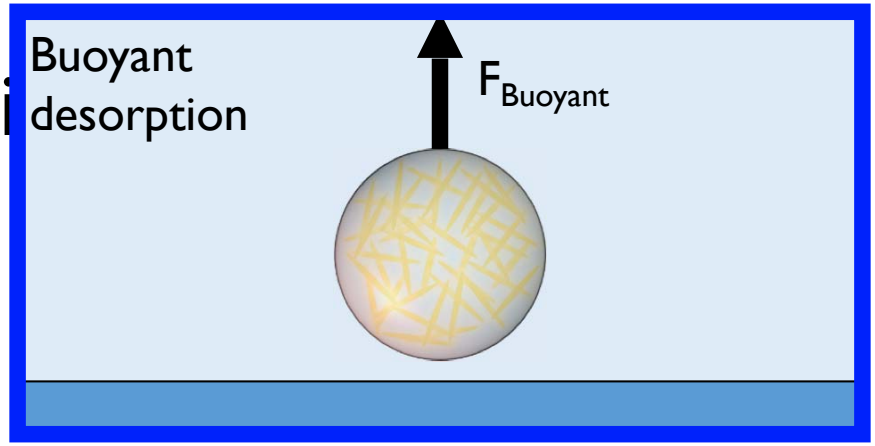
Buoyant
desorption
$F_{Buoyant}$

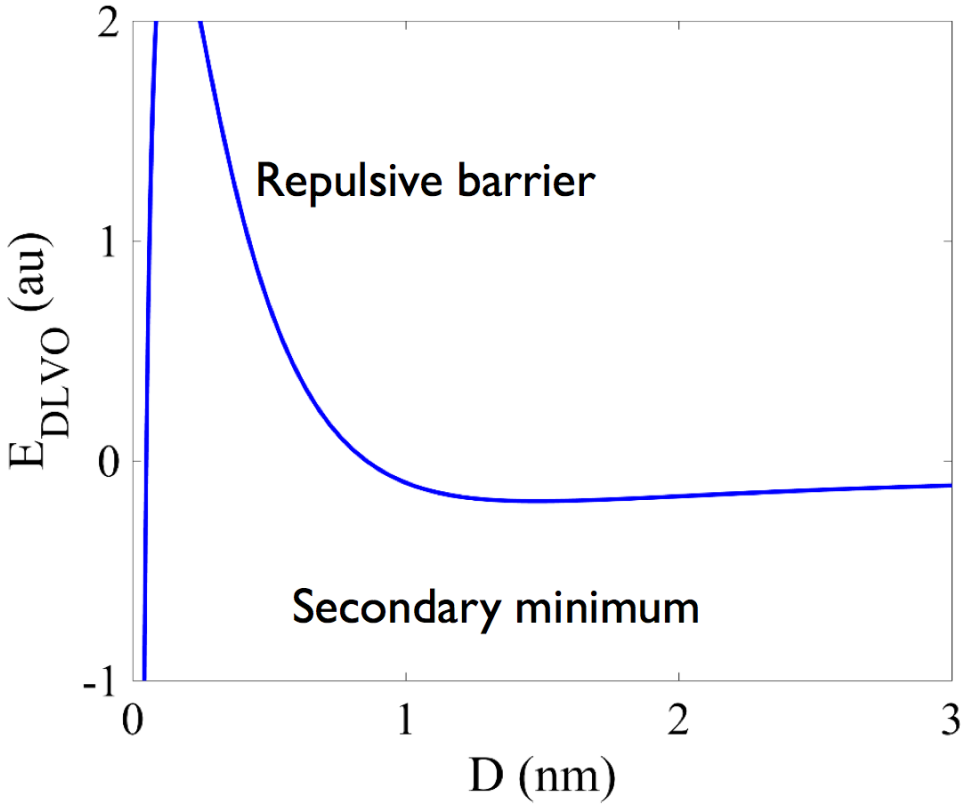
Repulsive barrier
Secondary minimum
E_{DLVO} (au)
D (nm)
2
1
0
-1
0
1
2
3

Depositi

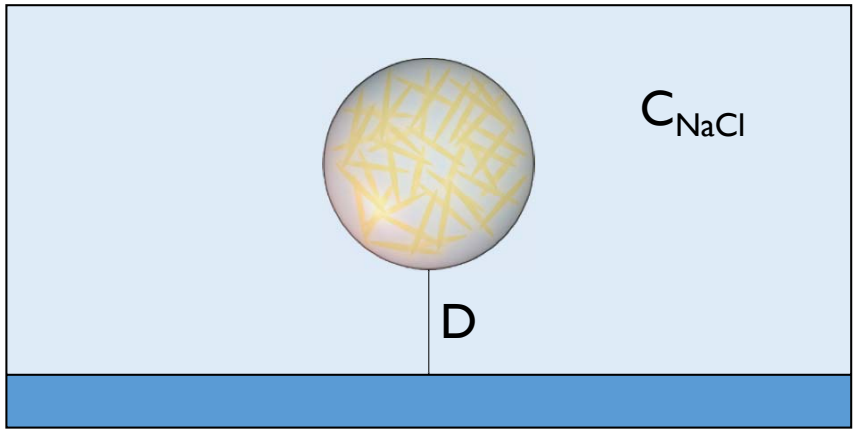
C_{NaCl}
D

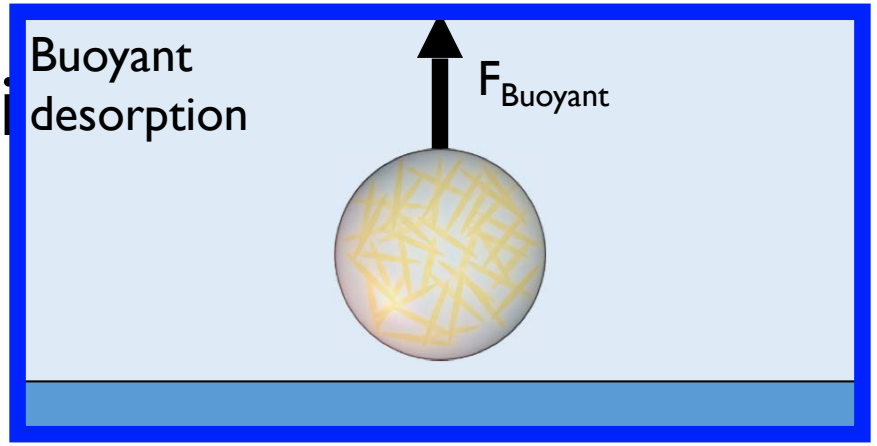
Buoyant
desorption
$F_{Buoyant}$

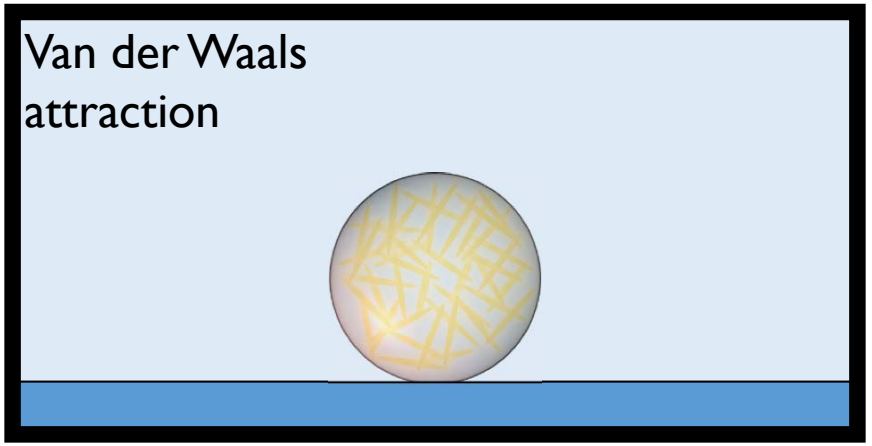
Van der Waals
attraction

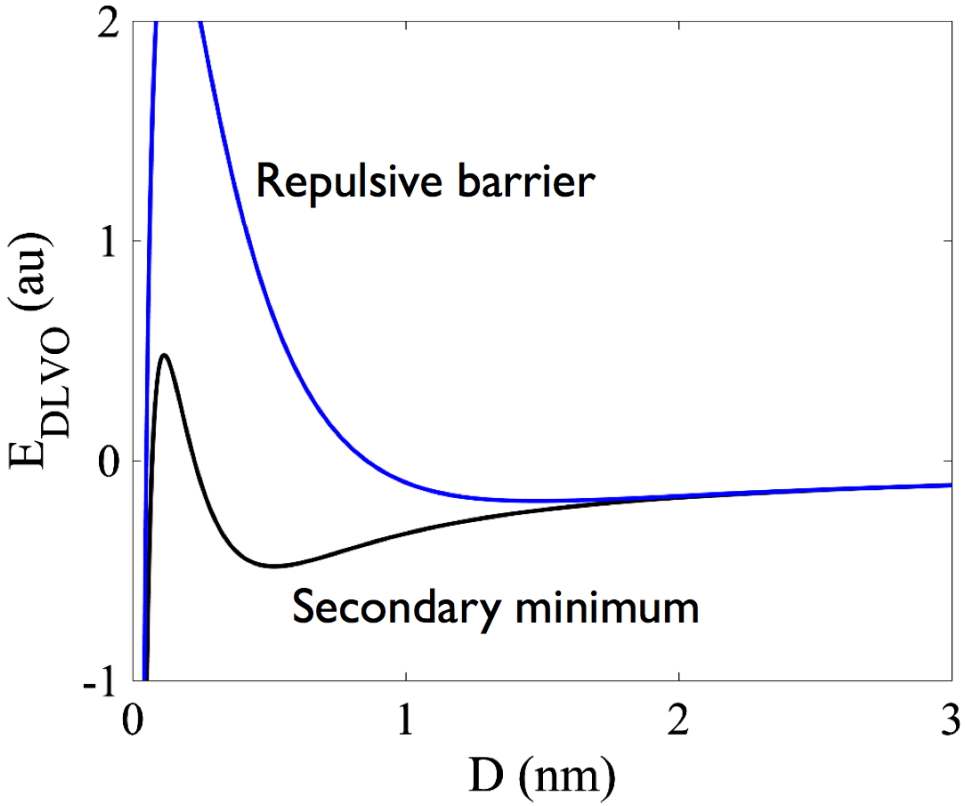
2
1
0
-1
E_{DLVO} (au)
Repulsive barrier
Secondary minimum
0
1
2
3
D (nm)

Depositi

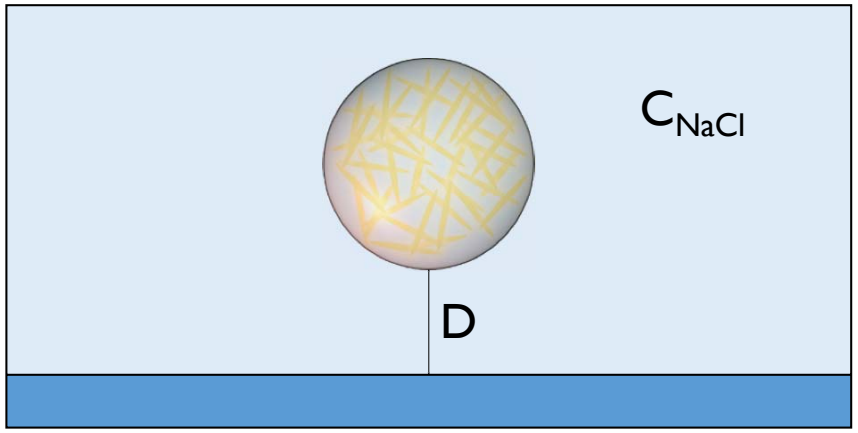
C_{NaCl}
D

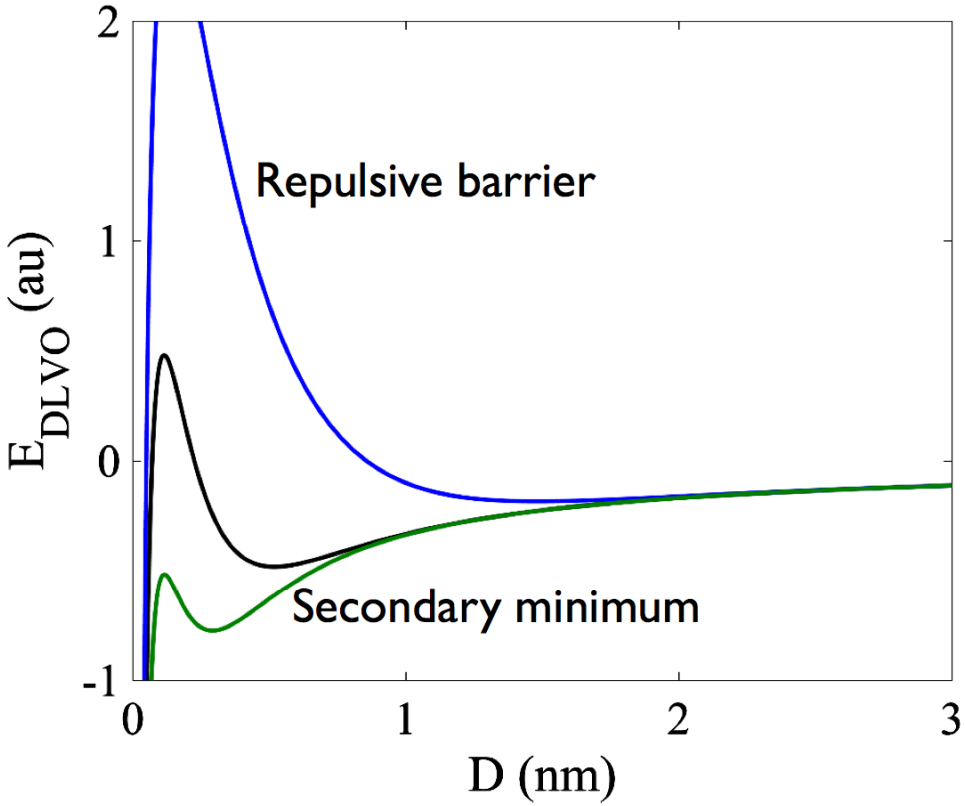
2
1
0
-1
E_{DLVO} (au)
Repulsive barrier
Secondary minimum
0
1
2
3
D (nm)

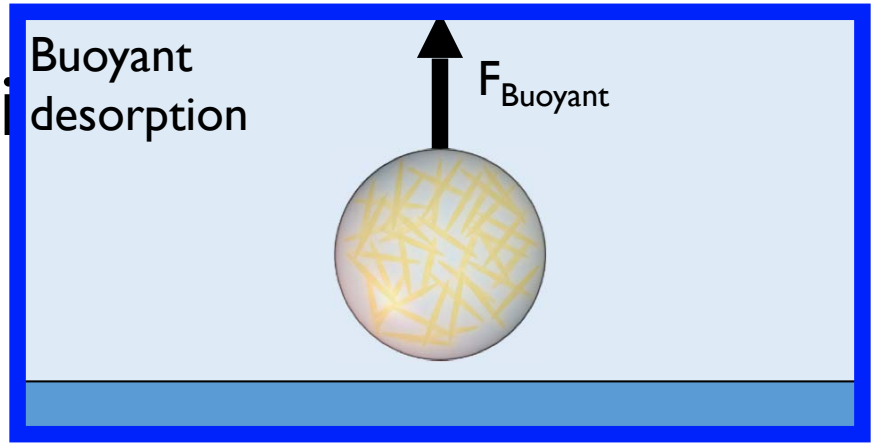
Buoyant desorption
$F_{Buoyant}$

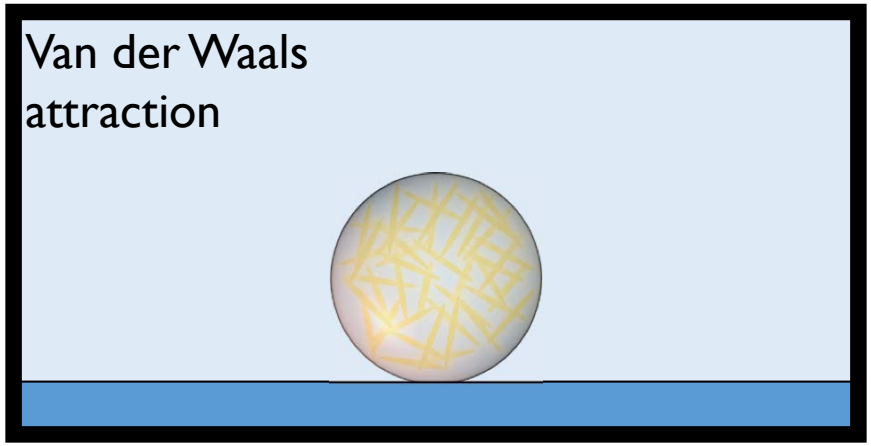
Van der Waals attraction

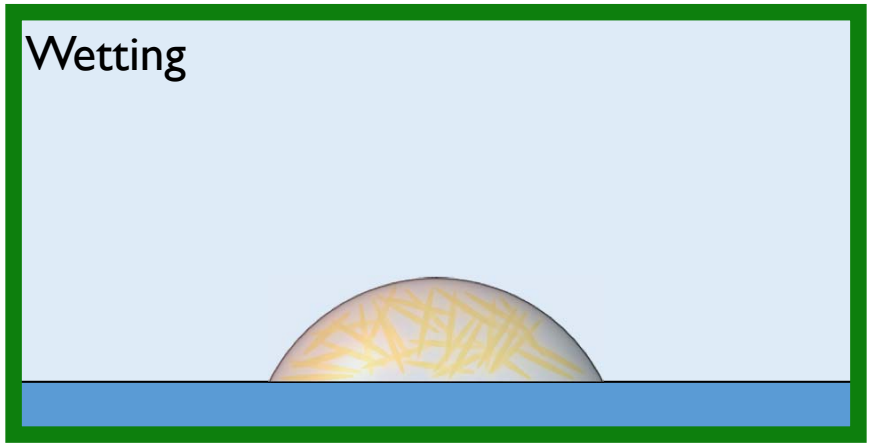
Wetting

Effect of shape on DLVO potential

Torres-Díaz, I. & Bevan, M. A. *Langmuir*. (2017)

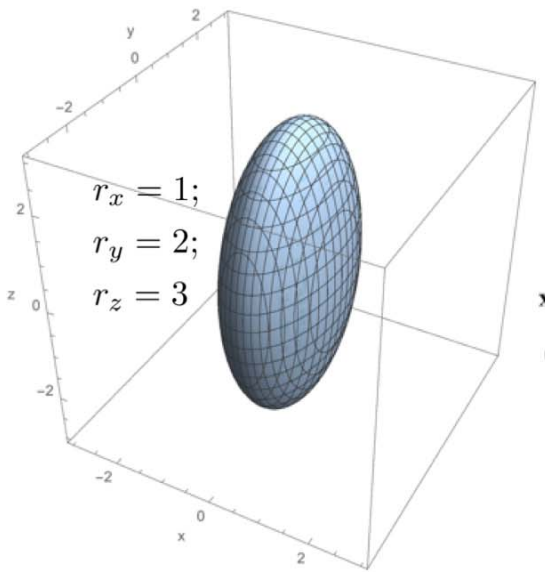

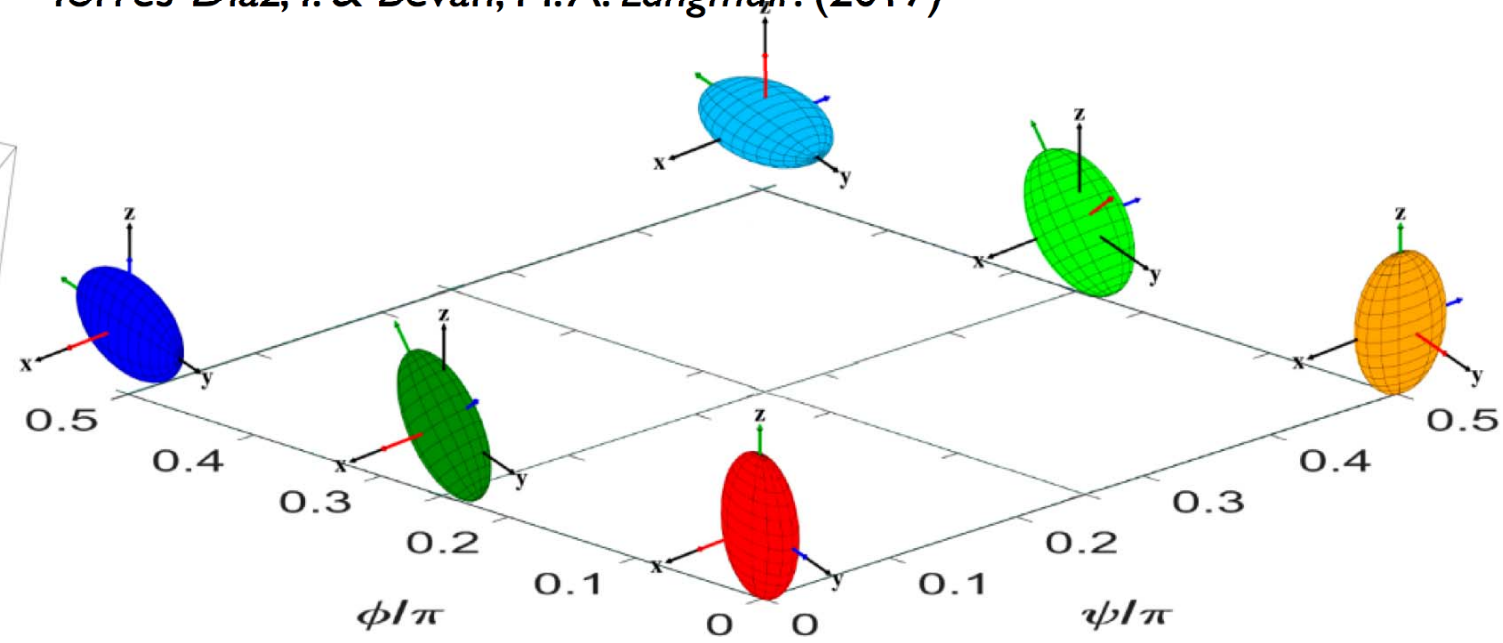

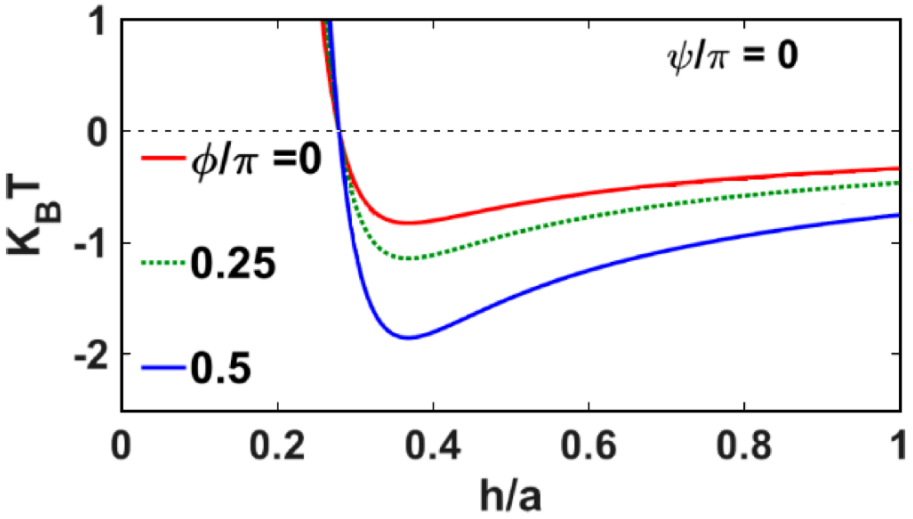

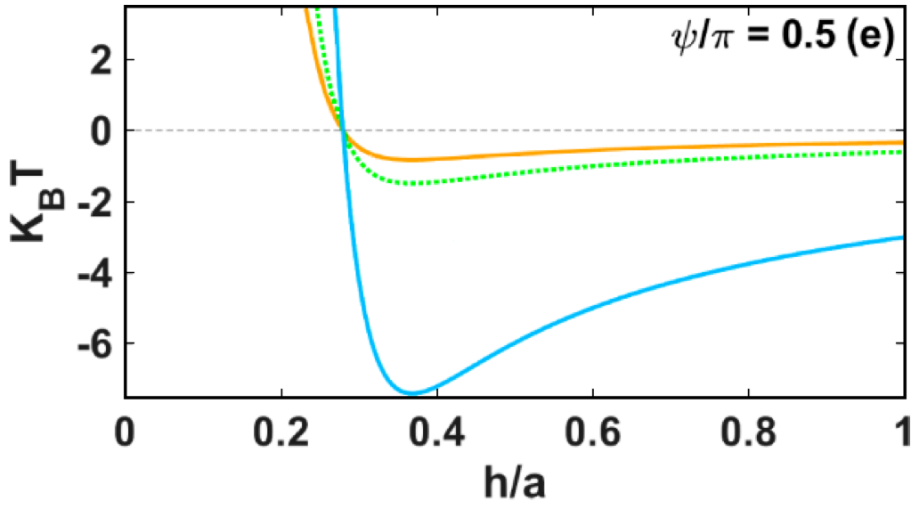

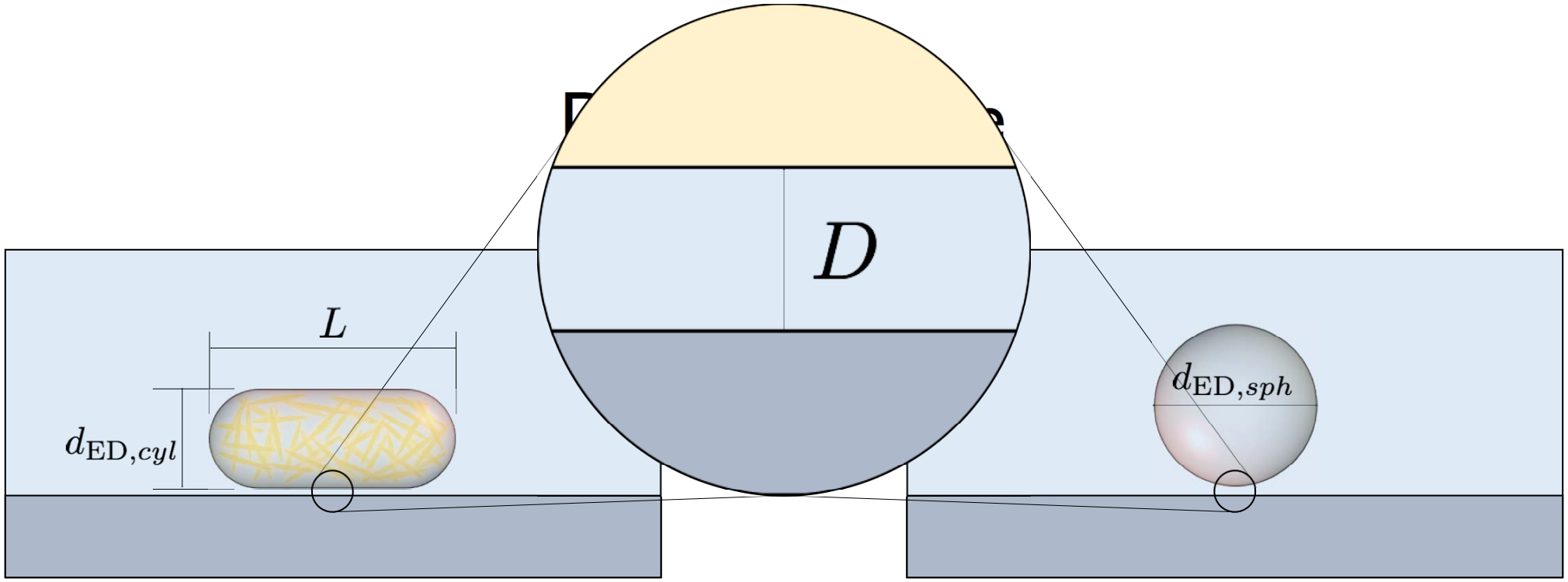
D
L
$d_{\mathrm{ED},cyl}$
$d_{\mathrm{ED},sph}$

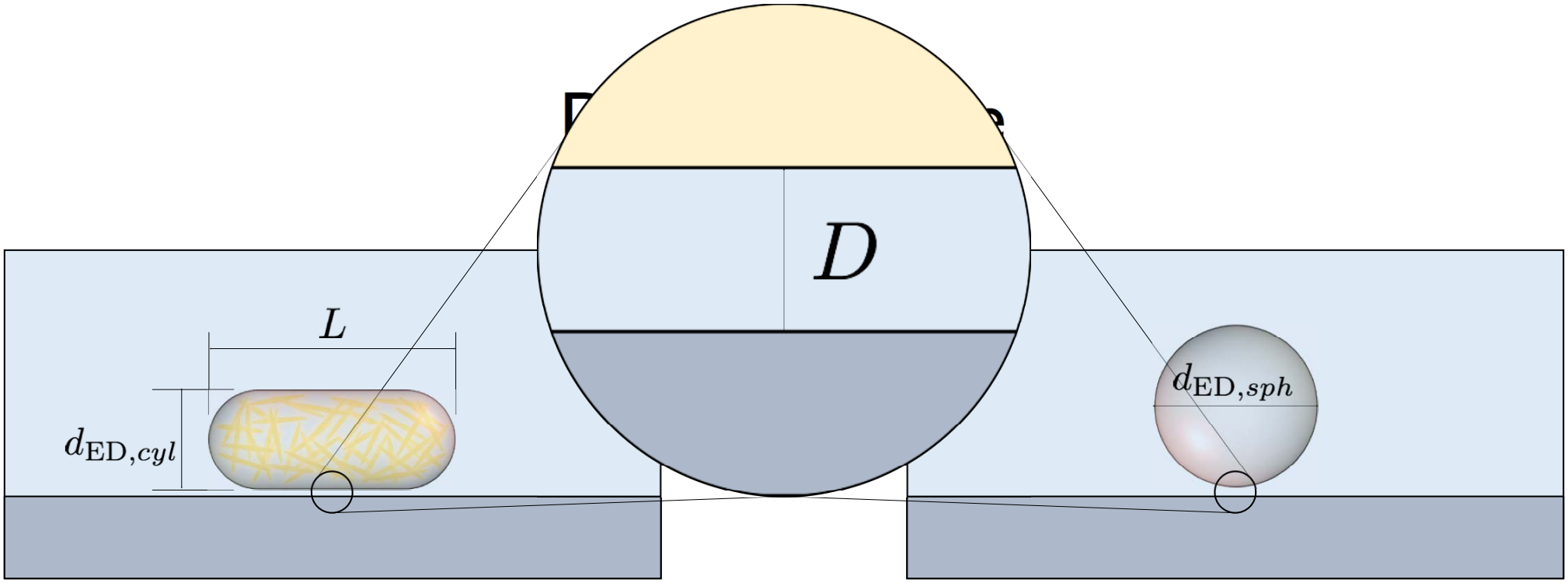

$$F_{\mathrm{B}} = V_{\mathrm{ED}} \left(\rho_{\mathrm{ED}} - \rho_{\mathrm{W}} \right) g$$

$$F_{\mathrm{B}} = \mathcal{O}(10^{-12}) \ \mathrm{N}$$

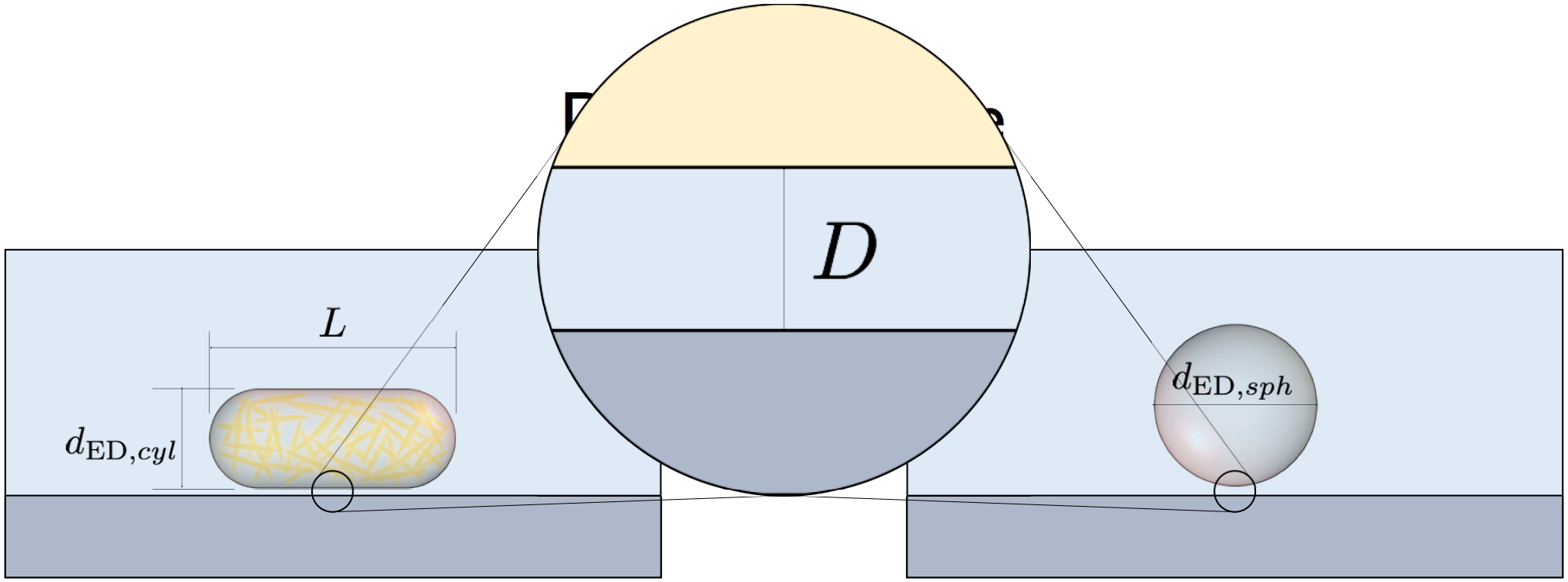

$$F_{\mathrm{B}} = V_{\mathrm{ED}} \left(\rho_{\mathrm{ED}} - \rho_{\mathrm{W}} \right) g$$

$$F_{\mathrm{B}} = \mathcal{O}(10^{-12}) \text{ N}$$

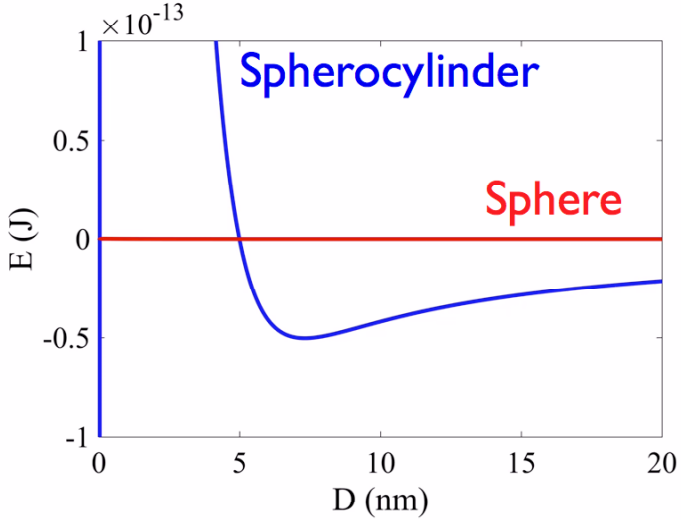

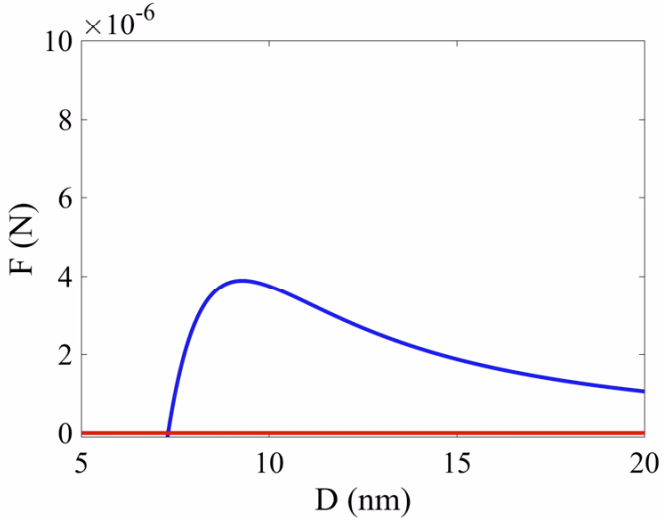

Spherocylinder

$$F_{\mathrm{max,SE}} = \mathcal{O}(10^{-6}) \text{ N}$$

Sphere

$$F_{\mathrm{max,S}} = \mathcal{O}(10^{-11}) \text{ N}$$

Some opportunities

Patrick Spicer (UNSW) & Tim Atherton (Tufts)

Dahiya, P. et al. *Soft Matter* 13, 2686–2697 (2017).

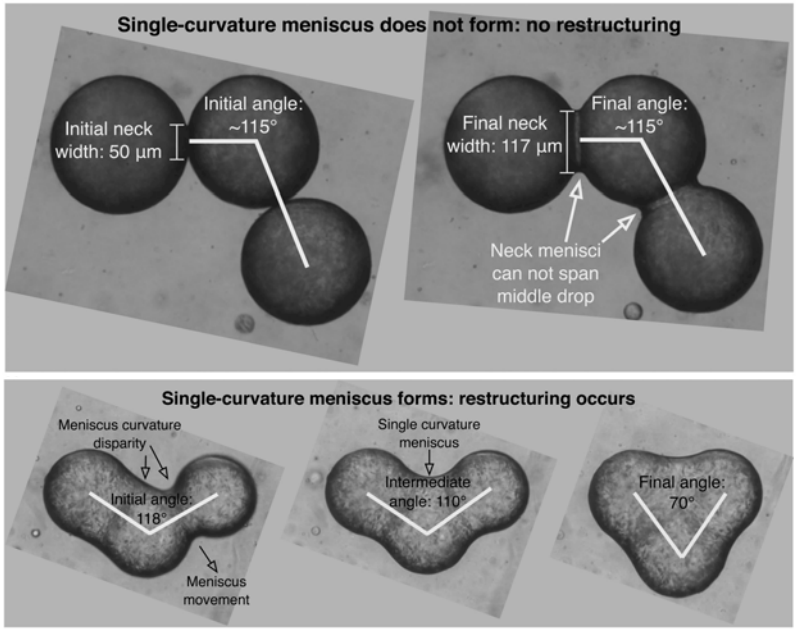

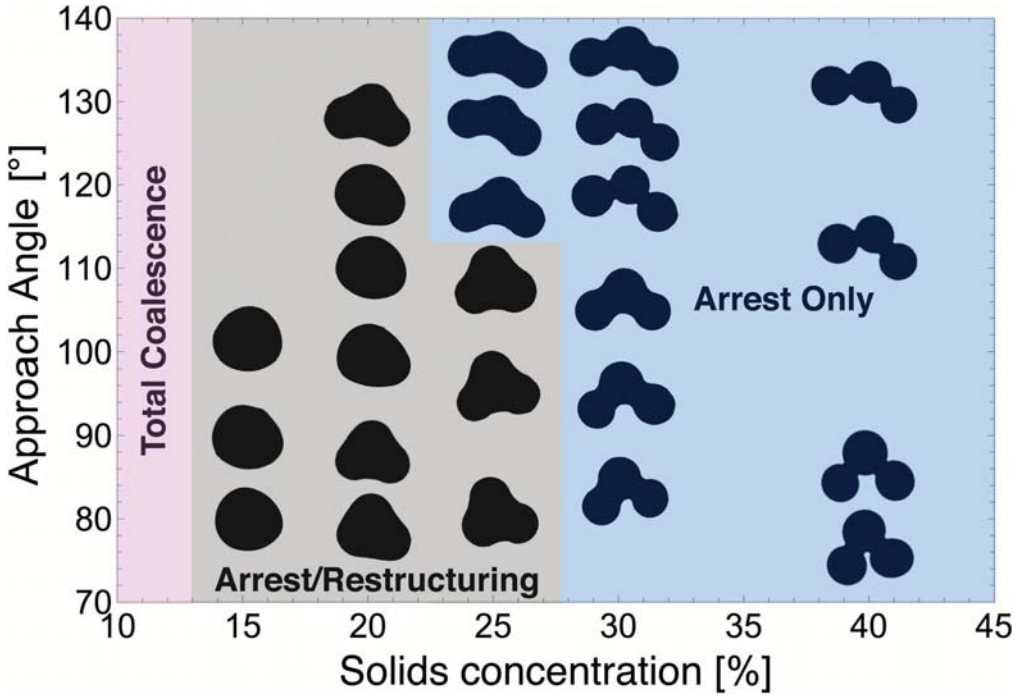

- Models of fluid interface and traction
- Engineering the fluid meniscus – rheology?

Wetting and spreading of structured droplets on surfaces

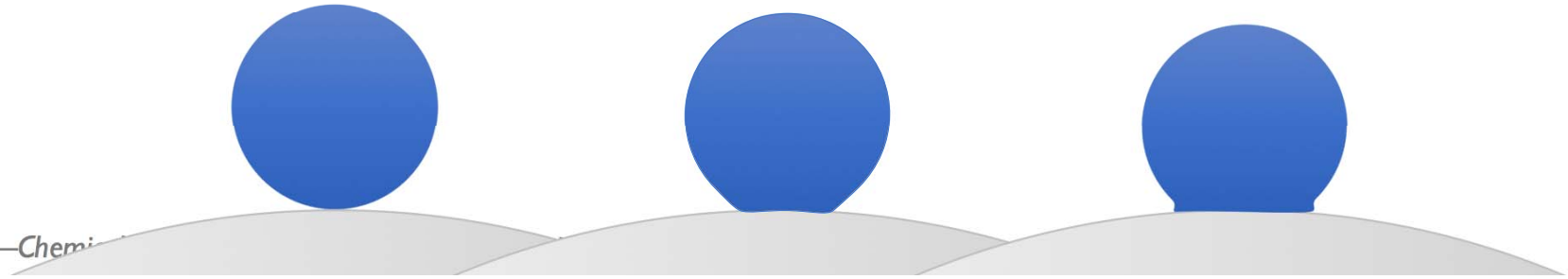

Some opportunities

Curvature-driven capillary migration and assembly of particles

Cavallaro, M. J., Botto, L., Lewandowski, E. P., Wang, M. & Stebe, K. J. *Proc. Natl. Acad. Sci. USA* 108, 20923–20928 (2011).

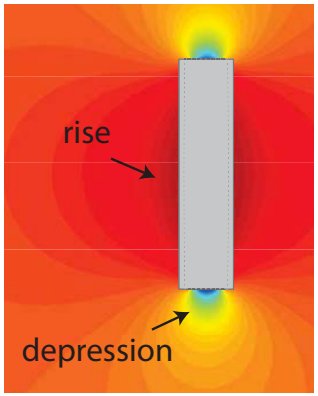

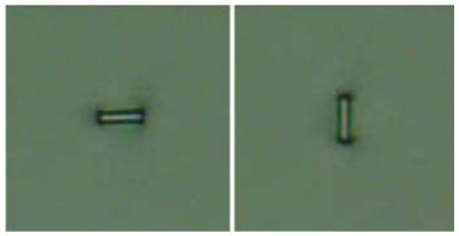

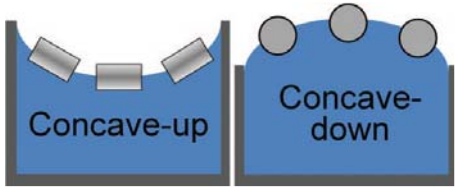

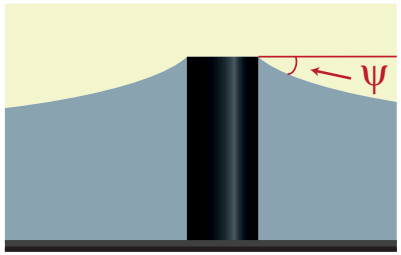

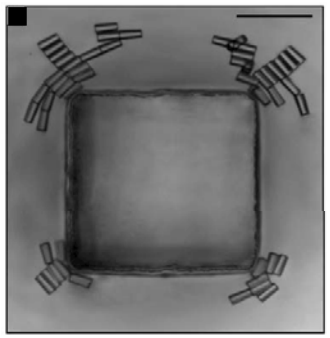

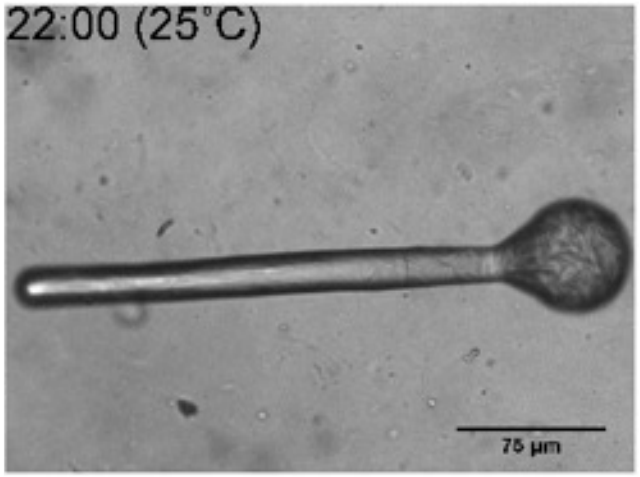

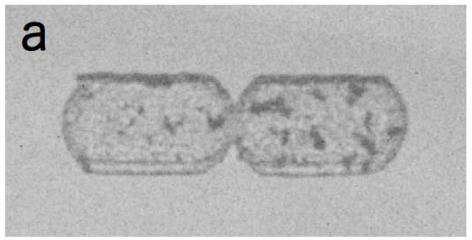

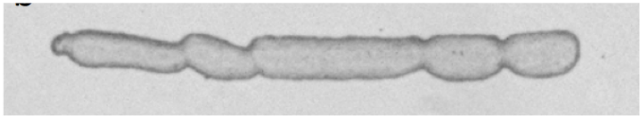

Fluid interfaces with complex shapes

…and challenges

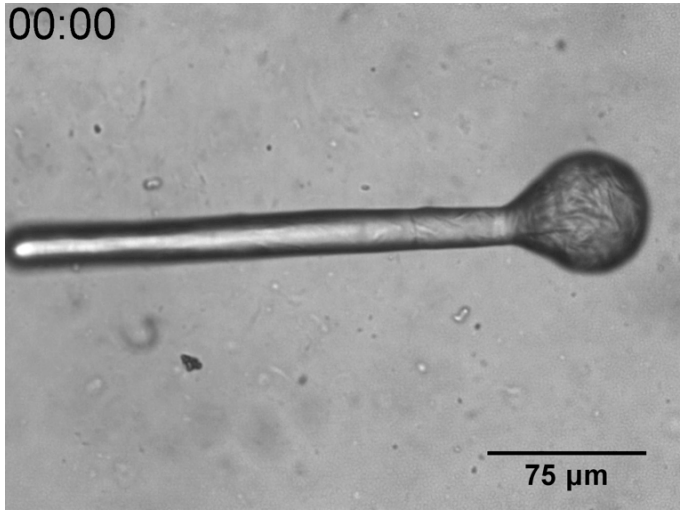

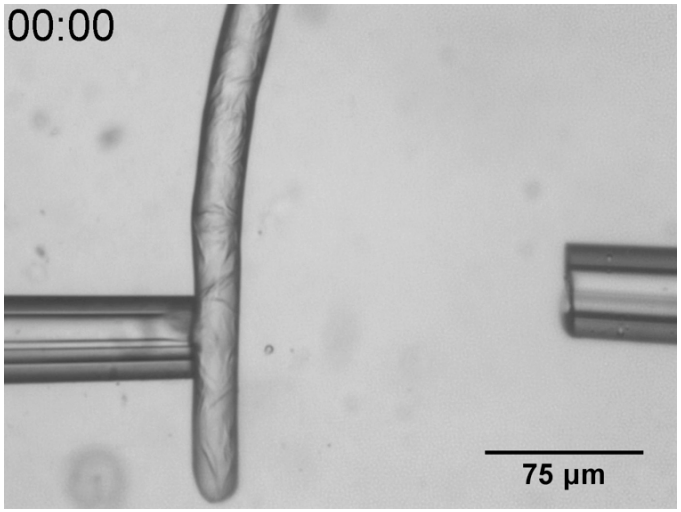

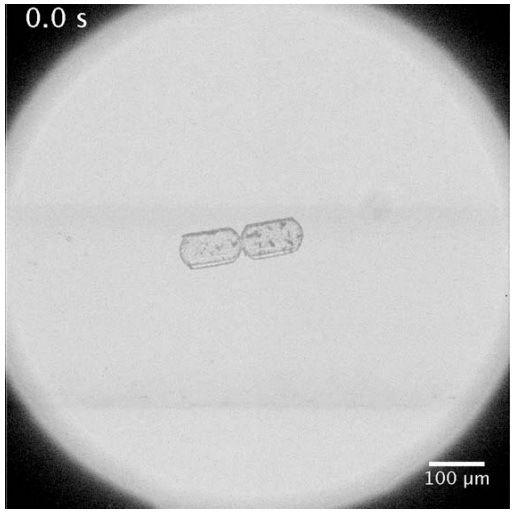

Reconfigurability is one-way, like:

Limulus acrosomal process, phage DNA delivery

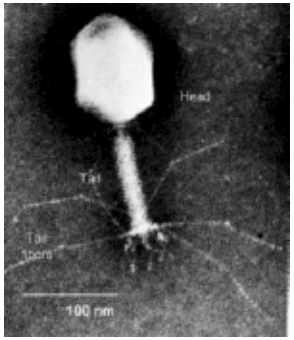

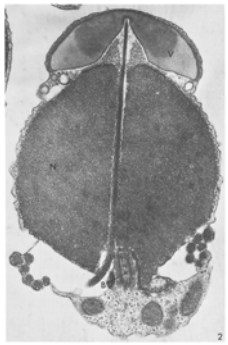

but unlike:

actin polymerization /
depolymerization driving cell motility

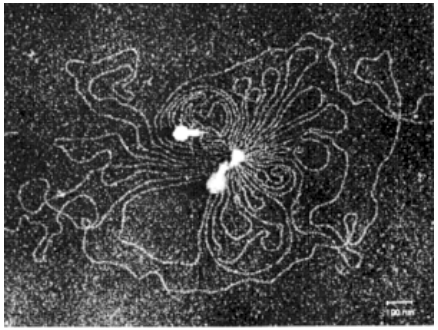

Endoskeletal droplets


Tamás Prileszky

Alexandra Bayles

Caggioni, M., Bayles, A.V, Lenis, J., Furst, E. M. & Spicer, P.T. *Soft Matter* 10, 7647–7652 (2014).
Caggioni, M., Lenis, J., Bayles, A.V., Furst, E. M. & Spicer, P.T. *Langmuir* 31, 8558–8565 (2015).

Microfluidics, hierarchical assembly

Prileszky, T.A. & Furst, E. M., *Chem. Mater.* 28, 3734–3740 (2016).
Prileszky, T.A. & Furst, E. M., *Langmuir* 32, 5141–5146 (2016).
Prileszky, T.A., Oggunaike, B.A. & Furst, E. M., *AIChE J.* 62, 2923–2928 (2016).

"Programmed" reconfigurability and response

Bayles, A.V., Prileszky, T.A., Spicer, P.T., & Furst, E. M. *Langmuir*, 34, 4116–4121 (2018).

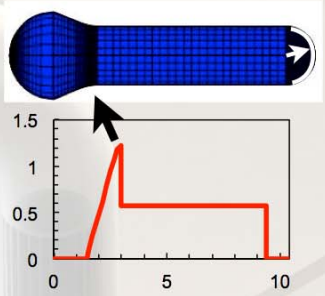

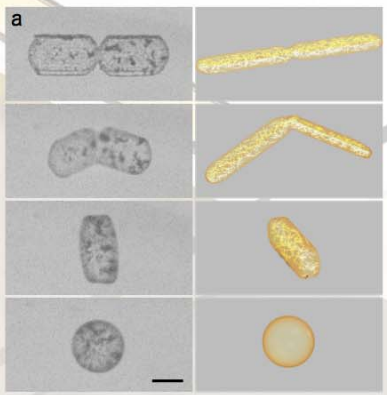

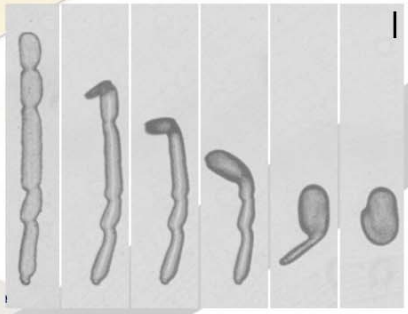

Procter & Gamble
NSF CBET-1336132

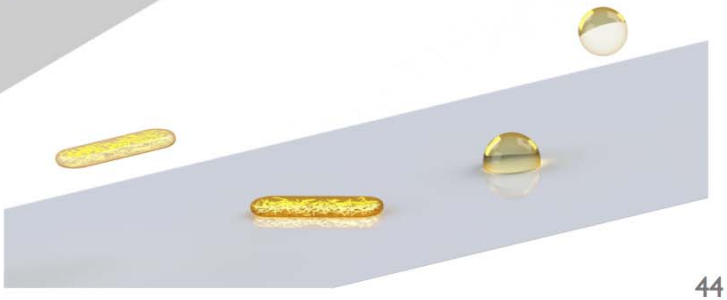

urst@udel.edu

Fluid interface
Held by endoskeleton
Thanks, biology!